eprints@whiterose.ac.uk
https://eprints.whiterose.ac.uk/

Thermal expectation values of fermions on anti-de Sitter space-time

Victor E. Ambruş

Department of Physics, West University of Timișoara, Bd. Vasile Pârvan 4, Timișoara 300223, Romania

E-mail: `Victor.Ambrus@e-uvt.ro`

Elizabeth Winstanley

Consortium for Fundamental Physics, School of Mathematics and Statistics, University of Sheffield, Hicks Building, Hounsfield Road, Sheffield. S3 7RH United Kingdom

E-mail: `E.Winstanley@sheffield.ac.uk`

Abstract. Making use of the symmetries of anti-de Sitter space-time, we derive an analytic expression for the bispinor of parallel transport, from which we construct in closed form the vacuum Feynman Green's function of the Dirac field on this background. Using the imaginary time anti-periodicity property of the thermal Feynman Green's function, we calculate the thermal expectation values of the fermion condensate and stress-energy tensor and highlight the effect of quantum corrections as compared to relativistic kinetic theory results.

1. Introduction

The formulation of the adS/CFT (anti-de Sitter space-time/conformal field theory) correspondence [1] sparked an explosion of interest in the behaviour of classical and quantum fields on asymptotically adS space-times (see, for example [2] for a review). In an appropriate limit, it is anticipated that results derived in a full theory of quantum gravity should reduce to those obtained within the semi-classical framework of quantum field theory (QFT) in curved space-time. In this setting, the space-time geometry is fixed and purely classical, with a quantum field propagating on this space-time background. Since the simplest asymptotically adS space-time is pure adS itself, a first step in understanding the behaviour of quantum fields on asymptotically adS geometries is to study quantum fields on pure adS space-time.

The fact that adS space-time is a maximally symmetric space-time simplifies many aspects of QFT on this classical background. At the same time, adS space-time is not globally hyperbolic, since it possesses closed time-like curves. While the closed time-like curves can be removed by considering the covering space of adS space-time, this is still not globally hyperbolic, which complicates QFT on this background. As a result, boundary conditions have to be applied on the time-like boundary [3] in order for the resulting QFT to be well-defined.

Quantum fields on four-dimensional adS space-time were first studied in [3], where a scalar field with arbitrary mass and general coupling to the space-time curvature is considered and closed-form expressions for the scalar field modes and the Feynman Green's function are derived. This work was extended to n-dimensional adS space-time in [4]. When the quantum scalar field is in the global adS vacuum state, the Feynman Green's function can be used to derive the renormalized vacuum expectation values (v.e.v.s) of the square of the scalar field and the stress-energy tensor (SET) using Hadamard renormalization [5] (these quantities can also be calculated using zeta-function regularization [6, 7]). Thermal expectation values (t.e.v.s) for a massless, conformally coupled scalar field on four-dimensional adS space-time have also been computed [8].

The maximal symmetry of adS space-time also simplifies the study of higher-spin fields, again allowing closed-form expressions for the Feynman Green's function to be derived in both the bosonic [9, 10] and fermionic [11, 12] cases. The field modes for a massive fermion field can also be found in closed form using a suitable choice of tetrad basis vectors [13]. For a massive fermion field on four-dimensional adS space-time, renormalized v.e.v.s of the fermion condensate (FC) and SET have been computed using various regularization techniques: Pauli-Villars, zeta-function [6] and Schwinger-de Witt, Hadamard [14], when the quantum field is in the global adS vacuum state. On the time-like space-time boundary, regular boundary conditions are imposed in [14], which correspond to the reflective boundary conditions in [3] for the scalar field case. The v.e.v.s for both scalar [5, 6, 7] and fermion [6, 14] fields on adS space-time have recently found application in a one-loop test of gauge-gravity duality [15].

In this paper we calculate t.e.v.s for a massive quantum fermion field on a four-dimensional adS space-time background, extending the work of [8] to a higher-spin field. As in [8], the regular boundary conditions imposed on the fermion field allow adS space-time to act like a perfectly reflecting box, and to be filled with thermal radiation. Due to the curvature of the space-time, the local temperature [16] of the radiation is not constant, and this breaks some of the space-time symmetries. The authors of [8] consider only a massless, conformally coupled scalar field, which means that the short-distance singularity structure of the vacuum Feynman Green's function possesses only poles, and no logarithmic singularities [17]. This enables them to use an elegant method to compute the t.e.v.s, by writing the thermal Feynman Green's function (which is doubly-periodic on pure adS space-time with closed time-like curves) in terms of an elliptic function. For a massive fermion field, in general the vacuum Feynman Green's

function has logarithmic short-distance singularities [14] and therefore the method in [8] cannot be extended to our situation. Nonetheless, we are able to derive closed-form expressions for the t.e.v.s of the FC and SET on adS space-time. We consider the differences in expectation values between the thermal state and the vacuum state, which do not require renormalization. The v.e.v.s derived in [14] could be added to the differences computed here to find the renormalized t.e.v.s. Remarkably, the quantum SET we compute here for the Dirac field takes the form of an ideal fluid, while the quantum SET for the Klein-Gordon field does not [8].

Recently, the energy density and pressure of a relativistic thermal gas of particles on adS space-time have been derived using kinetic theory, by solving the relativistic Boltzmann equation [18]. Using Maxwell-Jüttner statistics (the results can be extended to Bose-Einstein and Fermi-Dirac statistics following [19, 20]), it is found that the energy density and pressure depend only on the local temperature of the gas. For a massless, conformally coupled scalar field, this property is not shared by the quantum t.e.v.s [8]. We therefore compare our fermion quantum t.e.v.s with the results of classical relativistic kinetic theory, to examine the effect of quantum corrections.

The structure of the paper is as follows. In section 2, we review the Dirac equation on curved space-times and introduce our notation before describing, in section 3, those geometric properties of adS space-time relevant to our work. Section 4 contains a discussion of parallel transport on adS space-time using the bivector (for tensors) and bispinor (for spinors) of parallel transport, for which we present analytic expressions. In section 5, we review the construction of the vacuum Feynman Green's function for a Dirac field on adS space-time following [12, 14]. The computation of QFT t.e.v.s is performed in section 6, while the corresponding expressions in relativistic kinetic theory are obtained in section 7. In section 8, we compare the QFT t.e.v.s with the results from relativistic kinetic theory. Finally, our conclusions are presented in section 9.

2. Dirac equation on curved space-times

In this section we briefly review the formalism for Dirac spinors on a general curved space-time (see, for example, [21] for more details).

The Dirac equation for fermions of mass m which is covariant with respect to general coordinate transformations takes the form:

$$(i\gamma^{\hat{\alpha}} D_{\hat{\alpha}} - m)\psi(x) = 0, \tag{2.1}$$

where $\psi(x)$ is a spinor with four components. Throughout this paper, we use the mostly + convention for the metric signature and Planck units such that $G = c = \hbar = k_B = 1$.

In (2.1), hatted indices denote tensor components with respect to an orthonormal tetrad, comprising the frame vectors $e_{\hat{\alpha}} = e_{\hat{\alpha}}^{\mu} \partial_{\mu}$ and coframe one-forms $\omega^{\hat{\alpha}} = \omega_{\mu}^{\hat{\alpha}} dx^{\mu}$, chosen such that:

$$g_{\mu\nu} = \eta_{\hat{\alpha}\hat{\rho}} \omega_{\mu}^{\hat{\alpha}} \omega_{\nu}^{\hat{\rho}}, \qquad \langle \omega^{\hat{\alpha}}, e_{\hat{\rho}} \rangle \equiv \omega_{\mu}^{\hat{\alpha}} e_{\hat{\rho}}^{\mu} = \delta^{\hat{\alpha}}{}_{\hat{\rho}}, \tag{2.2}$$

where $g_{\mu\nu}$ are the metric components of the background geometry, while $\eta_{\hat{\alpha}\hat{\rho}} = \text{diag}(-1, 1, 1, 1)$ is the Minkowski metric. We employ the Dirac representation for the gamma matrices $\gamma^{\hat{\alpha}}$, such that:

$$\gamma^{\hat{0}} = \begin{pmatrix} 1 & 0 \\ 0 & -1 \end{pmatrix}, \qquad \gamma^{\hat{i}} = \begin{pmatrix} 0 & \sigma_i \\ -\sigma_i & 0 \end{pmatrix}, \tag{2.3}$$

where σ_i are the Pauli matrices:

$$\sigma_1 = \begin{pmatrix} 0 & 1 \\ 1 & 0 \end{pmatrix}, \qquad \sigma_2 = \begin{pmatrix} 0 & -i \\ i & 0 \end{pmatrix}, \qquad \sigma_3 = \begin{pmatrix} 1 & 0 \\ 0 & -1 \end{pmatrix}. \tag{2.4}$$

The gamma matrices satisfy the canonical anticommutation relations:

$$\{\gamma^{\hat{\alpha}}, \gamma^{\hat{\rho}}\} \equiv \gamma^{\hat{\alpha}}\gamma^{\hat{\rho}} + \gamma^{\hat{\rho}}\gamma^{\hat{\alpha}} = -2\eta^{\hat{\alpha}\hat{\rho}}. \tag{2.5}$$

The spinor covariant derivative

$$D_{\hat{\alpha}}\psi = e_{\hat{\alpha}}^{\mu}\partial_{\mu}\psi - \Gamma_{\hat{\alpha}}\psi \tag{2.6}$$

involves the spinor connection $\Gamma_{\hat{\alpha}}$, which has the following expression:

$$\Gamma_{\hat{\alpha}} = \frac{1}{2}\Gamma_{\hat{\rho}\hat{\sigma}\hat{\alpha}}\Sigma^{\hat{\rho}\hat{\sigma}}. \tag{2.7}$$

In (2.7), $\Sigma^{\hat{\rho}\hat{\sigma}}$ are the anti-Hermitian generators of Lorentz transformations:

$$\Sigma^{\hat{\rho}\hat{\sigma}} = \frac{1}{4}[\gamma^{\hat{\rho}}, \gamma^{\hat{\sigma}}], \tag{2.8}$$

while the connection coefficients $\Gamma_{\hat{\rho}\hat{\sigma}\hat{\alpha}}$ can be obtained using the following formula:

$$\Gamma_{\hat{\rho}\hat{\sigma}\hat{\alpha}} = \frac{1}{2}(c_{\hat{\rho}\hat{\sigma}\hat{\alpha}} + c_{\hat{\rho}\hat{\alpha}\hat{\sigma}} - c_{\hat{\sigma}\hat{\alpha}\hat{\rho}}). \tag{2.9}$$

The expression (2.9) is written in terms of the Cartan coefficients $c_{\hat{\alpha}\hat{\rho}}{}^{\hat{\sigma}}$, which can be obtained from the expression for the commutator of the tetrad vectors:

$$c_{\hat{\alpha}\hat{\rho}}{}^{\hat{\sigma}} = \langle\omega^{\hat{\sigma}}, [e_{\hat{\alpha}}, e_{\hat{\rho}}]\rangle \equiv \omega_{\mu}^{\hat{\sigma}}(e_{\hat{\alpha}}^{\nu}\partial_{\nu}e_{\hat{\rho}}^{\mu} - e_{\hat{\rho}}^{\nu}\partial_{\nu}e_{\hat{\alpha}}^{\mu}). \tag{2.10}$$

The classical fermion charge current (CC) has tetrad components

$$J^{\hat{\alpha}} = \overline{\psi}\gamma^{\hat{\alpha}}\psi, \tag{2.11}$$

where the conjugate spinor $\overline{\psi}$ is defined by $\overline{\psi} = \psi^{\dagger}\gamma^{\hat{0}}$. The classical SET for the spinor field has tetrad components [21]

$$T_{\hat{\alpha}\hat{\rho}} = \frac{i}{2}\left\{\overline{\psi}\gamma_{(\hat{\alpha}}D_{\hat{\rho})}\psi - \left[D_{(\hat{\alpha}}\overline{\psi}\right]\gamma_{\hat{\rho})}\psi\right\}, \tag{2.12}$$

where the covariant derivative of the conjugate spinor is

$$D_{\hat{\alpha}}\overline{\psi} = e_{\hat{\alpha}}^{\mu}\partial_{\mu}\overline{\psi} + \overline{\psi}\Gamma_{\hat{\alpha}}. \tag{2.13}$$

3. Geometry of anti-de Sitter space-time

Our focus in this paper is Dirac fermions on adS space-time. In this section we introduce the adS space-time metric, tetrad and connection coefficients, as well as the geodetic interval and its corresponding tangent vectors.

3.1. Coordinate system and metric

The adS space-time metric is given by:

$$ds^2 = \frac{1}{(\cos \omega r)^2} \left[-dt^2 + dr^2 + \left(\frac{\sin \omega r}{\omega} \right)^2 (d\theta^2 + \sin^2 \theta \, d\varphi^2) \right], \tag{3.1}$$

where ω is the inverse radius of curvature, $x^i = \{x, y, z\}$ and we use the standard spherical polar coordinates $\{r, \theta, \varphi\}$ with $r = \sqrt{x^2 + y^2 + z^2}$. While pure adS space-time is periodic in time t, in this paper we consider the covering space of adS, where $t \in (-\infty, \infty)$. The radial coordinate r is restricted to take values between $r = 0$ and $r = \pi/2\omega$, where the boundary of the space-time lies. The Ricci scalar for the metric (3.1) is $R = -12\omega^2$.

The metric (3.1) admits the following Cartesian-gauge tetrad [13]:

$$e_{\hat{0}} = \cos \omega r \, \partial_t, \qquad e_{\hat{i}} = \cos \omega r \left[\frac{\omega r}{\sin \omega r} \left(\delta_{ij} - \frac{x^i x^j}{r^2} \right) + \frac{x^i x^j}{r^2} \right] \partial_j, \tag{3.2}$$

$$\omega^{\hat{0}} = \frac{dt}{\cos \omega r}, \qquad \omega^{\hat{i}} = \frac{1}{\cos \omega r} \left[\frac{\sin \omega r}{\omega r} \left(\delta_{ij} - \frac{x^i x^j}{r^2} \right) + \frac{x^i x^j}{r^2} \right] dx^j. \tag{3.3}$$

The nonvanishing Cartan coefficients (2.10) corresponding to the tetrad (3.2–3.3) are:

$$c_{\hat{0}\hat{i}}{}^{\hat{0}} = \omega (\sin \omega r) \frac{x^i}{r}, \qquad c_{\hat{i}\hat{j}}{}^{\hat{k}} = -\omega \tan \frac{\omega r}{2} \left(\frac{x^i}{r} \delta_{jk} - \frac{x^j}{r} \delta_{ik} \right), \tag{3.4}$$

while the ensuing nonvanishing connnection coefficients (2.9) are:

$$\Gamma^{\hat{0}}{}_{\hat{i}\hat{0}} = \omega (\sin \omega r) \frac{x^i}{r}, \qquad \Gamma^{\hat{i}}{}_{\hat{j}\hat{k}} = -\omega \tan \frac{\omega r}{2} \left(\frac{x^i}{r} \delta_{jk} - \frac{x^j}{r} \delta_{ik} \right). \tag{3.5}$$

Finally, the spin connection coefficients $\Gamma_{\hat{\alpha}}$ (2.7) can be computed:

$$\begin{aligned} \Gamma_{\hat{0}} &= -\frac{\omega}{2} (\sin \omega r) \gamma^{\hat{0}} \left(\frac{\boldsymbol{x} \cdot \boldsymbol{\gamma}}{r} \right), \\ \Gamma_{\hat{k}} &= \frac{\omega}{2} \tan \frac{\omega r}{2} \left[\frac{x^k}{r} + \gamma^{\hat{k}} \left(\frac{\boldsymbol{x} \cdot \boldsymbol{\gamma}}{r} \right) \right], \end{aligned} \tag{3.6}$$

while their contraction with the γ matrices (2.3) reads:

$$\not{\Gamma} \equiv \gamma^{\hat{\alpha}} \Gamma_{\hat{\alpha}} = -\omega \tan \frac{\omega r}{2} \left(1 + \cos^2 \frac{\omega r}{2} \right) \left(\frac{\boldsymbol{x} \cdot \boldsymbol{\gamma}}{r} \right). \tag{3.7}$$

3.2. Geodesic structure

On adS, the geodetic interval $s(x, x')$ between two points $x = (t, \boldsymbol{x})$ and $x' = (t', \boldsymbol{x}')$ is given by the following relation [8]:

$$\cos(\omega s) = \frac{\cos \omega \Delta t}{\cos \omega r \cos \omega r'} - \cos \gamma \tan \omega r \tan \omega r', \tag{3.8}$$

where $\Delta t = t - t'$ and $\cos \gamma = \boldsymbol{x} \cdot \boldsymbol{x}'/rr'$ represents the cosine of the angle between $\boldsymbol{x}$ and $\boldsymbol{x}'$.

The tangent $n_\mu(x, x') = \nabla_\mu s(x, x')$ at x to the geodesic connecting the points x and x' has the following tetrad components

$$n_{\hat 0} = \frac{\sin \omega \Delta t}{\sin \omega s \cos \omega r'},$$

$$n_{\hat i} = -\frac{x^i}{r} \frac{\cos \omega \Delta t \sin \omega r - \cos \gamma \sin \omega r'(1 - \cos \omega r)}{\sin \omega s \cos \omega r \cos \omega r'} + \frac{\tan \omega r'}{\sin \omega s} \frac{x'^i}{r'}, \qquad (3.9)$$

while the components of the tangent $n_{\mu'}(x, x') = \nabla_{\mu'} s$ at x' can be obtained from (3.9) by swapping the coordinates x^μ and x'^μ. On maximally symmetric space-times, the tangents n_μ and $n_{\mu'}$ obey the following relations (which are not identical in form to those in [9] as we are using different conventions):

$$\nabla_{\hat\alpha} n_{\hat\rho} = -A(\eta_{\hat\alpha\hat\rho} + n_{\hat\alpha} n_{\hat\rho}), \qquad (3.10)$$

$$\nabla_{\hat\alpha'} n_{\hat\rho} = -C(g_{\hat\alpha'\hat\rho} - n_{\hat\alpha'} n_{\hat\rho}), \qquad (3.11)$$

$$\nabla_{\hat\sigma} g_{\hat\alpha\hat\rho'} = -(A + C)(\eta_{\hat\sigma\hat\alpha} n_{\hat\rho'} + g_{\hat\sigma\hat\rho'} n_{\hat\alpha}), \qquad (3.12)$$

where A and C are given on adS by [9]:

$$A = \omega \cot \omega s, \qquad C = -\frac{\omega}{\sin \omega s}, \qquad (3.13)$$

and $g_{\hat\alpha\hat\rho'}$ is the bivector of parallel transport, which will be introduced in the next section.

4. Parallel transport on adS space-time

In order to compute t.e.v.s in section 6, we first require the vacuum Feynman Green's function for the Dirac field $S_F(x, x')$, which we construct in section 5. The form of $S_F(x, x')$ derived in [12] involves the bispinor of parallel transport $\Lambda(x, x')$ (see (5.2)). The t.e.v. of the SET (6.3) also requires the bivector of parallel transport $g_{\mu\nu'}$. In this section we therefore derive analytic expressions for the bivector and bispinor of parallel transport on adS space-time.

4.1. Bivector of parallel transport

The bivector of parallel transport $g_{\mu\nu'}(x, x')$ is defined such that it performs the parallel transport of a tensor index ν' from x' to x. For example, for a vector field $V^{\mu'}(x')$, the following relation holds [22]:

$$V_\parallel^\mu(x) = g^\mu{}_{\nu'} V^{\nu'}(x'), \qquad (4.1)$$

where $V_\parallel^\mu(x)$ represents the vector $V^{\nu'}(x')$ evaluated at x', which is then parallel-transported to x along the geodesic connecting these two points. Thus $g_{\mu\nu'}$ satisfies the parallel transport equation [23]:

$$n^\lambda \nabla_\lambda g_{\mu\nu'} = 0, \qquad n^{\lambda'} \nabla_{\lambda'} g_{\mu\nu'} = 0, \qquad (4.2)$$

where the last equation is a statement that $g_{\mu\nu'}$ performs parallel transport both ways (from x to x', as well as from x' to x). The bivector of parallel transport also satisfies the conditions:

$$g^\mu{}_{\nu'} g^{\nu'}{}_\lambda = \delta^\mu{}_\lambda, \qquad g^{\mu'}{}_\lambda g^\lambda{}_{\nu'} = \delta^{\mu'}{}_{\nu'}. \qquad (4.3)$$

On adS space-time, (3.11) can be used to obtain an expression for the tetrad components $g_{\hat{\alpha}\hat{\rho}'}$ of the bivector of parallel transport:

$$g_{\hat{\alpha}'\hat{\rho}} = n_{\hat{\alpha}'}n_{\hat{\rho}} + \frac{\sin \omega s}{\omega} \nabla_{\hat{\alpha}'}n_{\hat{\rho}}. \tag{4.4}$$

Taking into account that all tetrad components (3.9) of $n_{\hat{\rho}}$ have a factor of $\sin \omega s$ in their denominator, it is convenient to introduce the reduced bivector of parallel transport $\widetilde{g}_{\hat{\alpha}'\hat{\rho}}$, defined by:

$$\widetilde{g}_{\hat{\alpha}'\hat{\rho}} = g_{\hat{\alpha}'\hat{\rho}} - n_{\hat{\alpha}'}n_{\hat{\rho}}(1 - \cos \omega s) = \frac{1}{\omega}\nabla_{\hat{\alpha}'}(n_{\hat{\rho}} \sin \omega s). \tag{4.5}$$

Since $n_{\hat{\rho}}(x, x')$ is a vector at x and a scalar at x', the covariant derivative $\nabla_{\hat{\alpha}'}$ acts as a simple differential operator:

$$\widetilde{g}_{\hat{\alpha}'\hat{\rho}} = \frac{1}{\omega}e^{\mu'}_{\hat{\alpha}'}\partial_{\mu'}[n_{\hat{\rho}}(x, x') \sin \omega s]. \tag{4.6}$$

The derivative with respect to x'^{μ} only acts on the primed coordinates in $n_{\hat{\rho}} \sin \omega s$. Working through the algebra, we find:

$$\widetilde{g}_{\hat{0}'\hat{0}} = -\cos \omega \Delta t,$$

$$\widetilde{g}_{\hat{0}'\hat{i}} = -\frac{x^i}{r} \sin \omega \Delta t \tan \omega r,$$

$$\widetilde{g}_{\hat{i}'\hat{0}} = \frac{x'^i}{r'} \sin \omega \Delta t \tan \omega r',$$

$$\widetilde{g}_{\hat{i}'\hat{j}} = \delta_{ij} + \frac{1 - \cos \omega r}{\cos \omega r}\frac{x^i x^j}{r^2} + \frac{1 - \cos \omega r'}{\cos \omega r'}\frac{x'^i x'^j}{(r')^2}$$
$$- \frac{x'^i x^j}{r' r}\left(\cos \omega \Delta t \tan \omega r \tan \omega r' - \cos \gamma \frac{1 - \cos \omega r}{\cos \omega r}\frac{1 - \cos \omega r'}{\cos \omega r'}\right), \tag{4.7}$$

from which it is straightforward to calculate $g_{\hat{\alpha}'\hat{\rho}}$ using (4.5).

4.2. Bispinor of parallel transport

In analogy to the role played by the bivector of parallel transport, the bispinor of parallel transport $\Lambda(x, x')$ performs the parallel transport of spinors, such that [12, 24, 25]:

$$\psi_{||}(x) = \Lambda(x, x')\psi(x'), \tag{4.8}$$

where $\psi_{||}(x)$ represents the spinor $\psi(x')$ evaluated at x', parallel-transported to x along the geodesic connecting these two points. The bispinor $\Lambda(x, x')$ must satisfy the parallel transport equations for spinors [12]:

$$n^{\hat{\alpha}}D_{\hat{\alpha}}\Lambda(x, x') = 0, \qquad n^{\hat{\alpha}'}D_{\hat{\alpha}'}\Lambda(x, x') = 0, \tag{4.9}$$

where

$$D_{\hat{\alpha}'}\Lambda(x, x') \equiv e^{\mu'}_{\hat{\alpha}'}\partial_{\mu'}\Lambda(x, x') + \Lambda(x, x')\Gamma_{\hat{\alpha}'}(x') \tag{4.10}$$

is the spinor covariant derivative of $\Lambda(x, x')$ with respect to the coordinate x'. The initial conditions for (4.9) are [12]:

$$\Lambda(x, x) = 1, \qquad \Lambda^{-1}(x, x') = \overline{\Lambda}(x, x') = \Lambda(x', x), \tag{4.11}$$

where the first equation implies that parallel transport from x to the same point x is the identity operation, while the second equation ensures that no parallel transport is performed on scalars of the form $\overline{\chi}\psi$. The parallel transport of the γ matrices is given by:

$$\Lambda(x, x')\gamma^{\mu'} = g^{\mu'}{}_{\nu}\gamma^{\nu}\Lambda(x, x'). \tag{4.12}$$

On adS space-time, equations (4.9, 4.12) can be used to obtain the following equations [12]:

$$D_{\hat{\alpha}}\Lambda(x, x') = -\frac{A + C}{2}(n_{\hat{\alpha}} + \gamma_{\hat{\alpha}}\slashed{n})\Lambda(x, x'),$$
$$D_{\hat{\alpha}'}\Lambda(x, x') = -\frac{A + C}{2}\Lambda(x, x')(n_{\hat{\alpha}'} + \slashed{n}'\gamma_{\hat{\alpha}'}), \tag{4.13}$$

where $\slashed{n} = \gamma^{\hat{\alpha}}n_{\hat{\alpha}}$. Using the expressions given in (3.13) for A and C, (4.13) can be written as:

$$D_{\hat{\alpha}}\Lambda(x, x') = \frac{\omega}{2}\tan\left(\frac{\omega s}{2}\right)(n_{\hat{\alpha}} + \gamma_{\hat{\alpha}}\slashed{n})\Lambda(x, x'),$$
$$D_{\hat{\alpha}'}\Lambda(x, x') = \frac{\omega}{2}\tan\left(\frac{\omega s}{2}\right)\Lambda(x, x')(n_{\hat{\alpha}'} + \slashed{n}'\gamma_{\hat{\alpha}'}). \tag{4.14}$$

Since constructing the solution $\Lambda(x, x')$ of (4.14) is a rather lengthy task, we simply present the result here and refer the reader to the Appendix for details of the derivation:

$$\Lambda(x, x') = \frac{\sec\frac{\omega s}{2}}{\sqrt{\cos\omega r\cos\omega r'}}\left[\cos\frac{\omega\Delta t}{2}\left(\cos\frac{\omega r}{2}\cos\frac{\omega r'}{2} + \sin\frac{\omega r}{2}\sin\frac{\omega r'}{2}\frac{\boldsymbol{x}\cdot\boldsymbol{\gamma}}{r}\frac{\boldsymbol{x}'\cdot\boldsymbol{\gamma}}{r'}\right)\right.$$
$$\left. + \sin\frac{\omega\Delta t}{2}\left(\sin\frac{\omega r}{2}\cos\frac{\omega r'}{2}\frac{\boldsymbol{x}\cdot\boldsymbol{\gamma}}{r}\gamma^{\hat{0}} + \sin\frac{\omega r'}{2}\cos\frac{\omega r}{2}\frac{\boldsymbol{x}'\cdot\boldsymbol{\gamma}}{r'}\gamma^{\hat{0}}\right)\right]. \tag{4.15}$$

In computing the t.e.v.s in section 6, we will require the quantity $\slashed{n}\Lambda$, which is also derived in the Appendix and given by:

$$\slashed{n}\Lambda(x, x')$$
$$= \frac{\operatorname{cosec}\frac{\omega s}{2}}{\sqrt{\cos\omega r\cos\omega r'}}\left[\sin\frac{\omega\Delta t}{2}\left(\cos\frac{\omega r}{2}\cos\frac{\omega r'}{2}\gamma^{\hat{0}} - \sin\frac{\omega r}{2}\sin\frac{\omega r'}{2}\frac{\boldsymbol{x}\cdot\boldsymbol{\gamma}}{r}\frac{\boldsymbol{x}'\cdot\boldsymbol{\gamma}}{r'}\gamma^{\hat{0}}\right)\right.$$
$$\left. - \cos\frac{\omega\Delta t}{2}\left(\sin\frac{\omega r}{2}\cos\frac{\omega r'}{2}\frac{\boldsymbol{x}\cdot\boldsymbol{\gamma}}{r} - \cos\frac{\omega r}{2}\sin\frac{\omega r'}{2}\frac{\boldsymbol{x}'\cdot\boldsymbol{\gamma}}{r'}\right)\right]. \tag{4.16}$$

5. Feynman Green's function for the global maximally-symmetric vacuum

In this section, we review the construction of the Feynman Green's function $S_F(x, x')$ for the global vacuum state of the Dirac field on adS space-time [12, 14].

The Feynman Green's function $S_F(x, x')$ satisfies the inhomogeneous Dirac equation:

$$\left(i\slashed{D} - m\right)S_F(x, x') = \frac{1}{\sqrt{-g}}\delta^4(x - x'). \tag{5.1}$$

Due to the maximal symmetry of adS space-time, the fermion Feynman Green's function $S_F(x, x')$ for the global adS vacuum state can be written as [12]:

$$iS_F(x, x') = (\mathcal{A}_F + \mathcal{B}_F\slashed{n})\Lambda(x, x'), \tag{5.2}$$

where $\mathcal{A}_F$ and $\mathcal{B}_F$ are scalar functions of the geodetic interval s. Substituting the ansatz (5.2) into (5.1) and using the properties (3.10, 4.14) of the derivatives of n_μ and $\Lambda(x, x')$, we can reduce (5.1) to two coupled equations:

$$i\omega \frac{\partial \mathcal{A}_F}{\partial (\omega s)} - \frac{3i\omega}{2} \mathcal{A}_F \tan\left(\frac{\omega s}{2}\right) - m\mathcal{B}_F = 0, \tag{5.3}$$

$$i\omega \frac{\partial \mathcal{B}_F}{\partial (\omega s)} + \frac{3i\omega}{2} \mathcal{B}_F \cot\left(\frac{\omega s}{2}\right) - m\mathcal{A}_F = \frac{i}{\sqrt{-g}} \delta(x, x'). \tag{5.4}$$

The solution of the system (5.3–5.4) can be written as [14]:

$$\mathcal{A}_F = \frac{\omega^3 \Gamma(2+k)}{16\pi^{\frac{3}{2}} 4^k \Gamma\left(\frac{1}{2}+k\right)} \cos\left(\frac{\omega s}{2}\right) \left[-\sin^2\left(\frac{\omega s}{2}\right)\right]^{-2-k}$$
$$\times {}_2F_1\left(1+k, 2+k; 1+2k; \operatorname{cosec}^2\left(\frac{\omega s}{2}\right)\right), \tag{5.5}$$

where k is given in terms of the fermion mass m and inverse radius of curvature ω by

$$k = \frac{m}{\omega} \tag{5.6}$$

and ${}_2F_1(a, b; c; z)$ is a hypergeometric function. Inserting the expression (5.5) for $\mathcal{A}_F$ in (5.3) gives:

$$\mathcal{B}_F = \frac{i\omega^3 \Gamma(2+k)}{16\pi^{\frac{3}{2}} 4^k \Gamma\left(\frac{1}{2}+k\right)} \sin\left(\frac{\omega s}{2}\right) \left[-\sin^2\left(\frac{\omega s}{2}\right)\right]^{-2-k}$$
$$\times {}_2F_1\left(k, 2+k; 1+2k; \operatorname{cosec}^2\left(\frac{\omega s}{2}\right)\right). \tag{5.7}$$

The expressions (5.5, 5.7) simplify considerably in the massless case ($k = 0$):

$$\mathcal{A}_F\rfloor_{k=0} = \frac{\omega^3}{16\pi^2}\left(\cos\frac{\omega s}{2}\right)^{-3}, \qquad \mathcal{B}_F\rfloor_{k=0} = \frac{i\omega^3}{16\pi^2}\left(\sin\frac{\omega s}{2}\right)^{-3}. \tag{5.8}$$

6. Thermal expectation values

We now have all the ingredients necessary for a computation of the t.e.v.s of the FC $\langle\overline{\psi}\psi\rangle$, CC $\langle J^{\hat{\alpha}}\rangle$ and SET $\langle T_{\hat{\alpha}\hat{\rho}}\rangle$ for a massive fermion field at inverse temperature β. The required quantities are: the exact expression (4.15) for the bispinor of parallel transport and the functions $\mathcal{A}_F$ (5.5) and $\mathcal{B}_F$ (5.7) necessary to construct the vacuum Feynman Green's function (5.2).

6.1. Finite temperature Feynman Green's function

The expectation values of the FC $\langle\overline{\psi}\psi\rangle$, CC $\langle J^{\hat{\alpha}}\rangle$ and SET $\langle T_{\hat{\alpha}\hat{\rho}}\rangle$ for a given state can be calculated from the Feynman Green's function $S_F(x, x')$ corresponding to that state using the following expressions [14, 25]:

$$\langle\overline{\psi}\psi\rangle = -\lim_{x'\to x} \operatorname{tr}\left[iS_F(x, x')\Lambda(x', x)\right], \tag{6.1}$$

$$\langle J^{\hat{\alpha}}\rangle = -\lim_{x'\to x} \operatorname{tr}\left[\gamma^{\hat{\alpha}} iS_F(x, x')\Lambda(x', x)\right], \tag{6.2}$$

$$\langle T_{\hat{\alpha}\hat{\rho}}\rangle = \frac{i}{2}\lim_{x'\to x} \operatorname{tr}\left\{\left[\gamma_{(\hat{\alpha}} D_{\hat{\rho})} iS_F(x, x') - D_{\hat{\rho}'}[iS_F(x, x')]\gamma_{\hat{\alpha}'} g^{\hat{\alpha}'}_{\ (\hat{\alpha}} g^{\hat{\rho}'}_{\ \hat{\rho})}\right]\Lambda(x', x)\right\}. \tag{6.3}$$

Taking the trace of (6.3), since the fermion Feynman Green's function satisfies the inhomogeneous Dirac equation (5.1), we find the following relation between the unrenormalized FC and the SET trace

$$\langle T^{\hat{\alpha}}_{\hat{\alpha}} \rangle = -m \langle \overline{\psi}\psi \rangle. \tag{6.4}$$

This relationship is not preserved during the renormalization process. In particular, (6.4) does not hold for the v.e.v.s of the FC and SET calculated in [14], regardless of the method of renormalization.

To compute the expectation values (6.1–6.3) at finite temperature, the thermal Feynman Green's function can be constructed as follows [26]:

$$S^{\beta}_F(x, x') = \sum_j (-1)^j S_F(t + ij\beta, \boldsymbol{x}; t', \boldsymbol{x}'), \tag{6.5}$$

where j runs over all integers, so that $S^{\beta}_F(x, x')$ is anti-periodic in imaginary time, with period β. It is convenient to introduce the following notation:

$$S^{\beta}_F(x, x') = \sum_j (-1)^j [\mathcal{A}_F(s_j) + \mathcal{B}_F(s_j)\slashed{n}_j]\Lambda_j(x_j, x'), \tag{6.6}$$

where the quantity s_j is the geodetic interval between the points $x_j = (t + ij\beta, \boldsymbol{x})$ and $x' = (t', \boldsymbol{x}')$, the vector n_j is the corresponding tangent vector and $\Lambda_j(x_j, x')$ is the bispinor of parallel transport between these two points.

The v.e.v.s of the FC, CC and SET when the fermion field is in the global adS vacuum were calculated in [14]. In this section we compute the difference between the t.e.v.s at finite inverse temperature β and the v.e.v.s. Since the short-distance singularity structure of the Feynman Green's function is independent of the state of the quantum field (see, for example, [14]), these differences do not require renormalization and the relationship (6.4) between the FC and the trace of the SET will hold.

The $j = 0$ term in (6.6) is the vacuum Feynman Green's function. Therefore, to find the differences between the t.e.v.s and the v.e.v.s, we simply subtract the $j = 0$ term from (6.6), and substitute into (6.1–6.3) as applicable. The bispinor of parallel transport written explicitly in (6.1–6.3) is between the points $x = (t, \boldsymbol{x})$ and $x' = (t', \boldsymbol{x}')$ as the shift $s \to s_j$ occurs only in the thermal Feynman Green's function (6.6). Since the quantities resulting from (6.1–6.3) do not require renormalization, we can then straightforwardly bring the space-time points together by setting $\boldsymbol{x}' = \boldsymbol{x}$ and $t' = t$. However, in doing so s_j will remain nonzero because it will be the geodetic interval between the points $x_j = (t + ij\beta, \boldsymbol{x})$ and $x = (t, \boldsymbol{x})$. Similarly, $\Lambda_j(x_j, x)$ will be nontrivial.

We use the notation $\langle : \overline{\psi}\psi : \rangle_\beta$, $\langle : J^{\hat{\alpha}} : \rangle_\beta$ and $\langle : T_{\hat{\alpha}\hat{\rho}} : \rangle_\beta$ to denote these differences in expectation values for the FC, CC and SET respectively. The full t.e.v.s for each quantity can easily be found from the results in this section by simply adding the v.e.v.s of the corresponding quantity from [14]‡.

‡ The renormalized expectation value of the FC reported in equations (38a, 51a) of [14] must be multiplied by -1.

6.2. Fermion condensate

Subtracting the $j = 0$ term from (6.6) and inserting into (6.1), the following expression is obtained for the difference between the t.e.v. and the v.e.v. of the FC:

$$FC_\beta = \langle : \overline{\psi}\psi : \rangle_\beta = -\sum_{j\neq 0}(-1)^j \lim_{\substack{\boldsymbol{x}'\to\boldsymbol{x} \\ \Delta t\to ij\beta}} \mathcal{A}_F(s_j)\mathrm{tr}[\Lambda_j(x_j, x')], \tag{6.7}$$

where we have set $\Lambda(x, x) = 1$ in (6.1). When $\boldsymbol{x}' = \boldsymbol{x}$, we find from (4.15) that:

$$\Lambda_j(x_j, x')\rfloor_{\boldsymbol{x}'=\boldsymbol{x}} = \frac{\sec\frac{\omega s_j}{2}}{\cos\omega r}\left(\cos\frac{\omega\Delta t_j}{2}\cos\omega r + \sin\frac{\omega\Delta t_j}{2}\sin\omega r\frac{\boldsymbol{x}\cdot\boldsymbol{\gamma}}{r}\gamma^{\hat{0}}\right), \tag{6.8}$$

where $\Delta t_j = t - t' + ij\beta$. The difference between the t.e.v. and the v.e.v. of the FC then becomes, using (5.5):

$$FC_\beta = \langle : \overline{\psi}\psi : \rangle_\beta = -\sum_{j\neq 0}(-1)^j\frac{\omega^3\cos\left(\frac{\omega\Delta t_j}{2}\right)\Gamma(2+k)}{\pi^{3/2}4^{1+k}\Gamma\left(\frac{1}{2}+k\right)}\left[-\sin^2\left(\frac{\omega s_j}{2}\right)\right]^{-2-k}$$

$$\times {}_2F_1\left(1+k, 2+k; 1+2k; \mathrm{cosec}^2\left(\frac{\omega s_j}{2}\right)\right). \tag{6.9}$$

To further simplify the above expression, the limit $\boldsymbol{x}' = \boldsymbol{x}$ of the geodetic interval (3.8) gives:

$$\cos\omega s_j\rfloor_{\boldsymbol{x}'=\boldsymbol{x}} = 1 - \frac{2\sin^2\frac{\omega\Delta t_j}{2}}{\cos^2\omega r}, \qquad \sin^2\frac{\omega s_j}{2}\bigg\rfloor_{\boldsymbol{x}'=\boldsymbol{x}} = \frac{\sin^2\frac{\omega\Delta t_j}{2}}{\cos^2\omega r}. \tag{6.10}$$

Setting $t' = t$, we then have $\Delta t_j = ij\beta$ and (6.9) reduces to:

$$FC_\beta = \langle : \overline{\psi}\psi : \rangle_\beta = -\frac{2\omega^3\Gamma(2+k)(\cos\omega r)^{4+2k}}{\pi^{3/2}4^{1+k}\Gamma(\frac{1}{2}+k)}\sum_{j=1}^{\infty}(-1)^j\frac{\cosh\frac{\omega j\beta}{2}}{(\sinh\frac{\omega j\beta}{2})^{4+2k}}$$

$$\times {}_2F_1\left(1+k, 2+k; 1+2k; -\frac{\cos^2\omega r}{\sinh^2\frac{\omega j\beta}{2}}\right). \tag{6.11}$$

In the massless case $(k = 0)$, this simplifies even further to the nonzero expression:

$$FC_\beta = \langle : \overline{\psi}\psi : \rangle_\beta = -\frac{\omega^3(\cos\omega r)^4}{2\pi^2}\sum_{j=1}^{\infty}(-1)^j\frac{\cosh\frac{\omega j\beta}{2}}{(\sinh^2\frac{\omega j\beta}{2} + \cos^2\omega r)^2}. \tag{6.12}$$

6.3. Charge current

The difference between the t.e.v. and the v.e.v. for the CC has the following expression:

$$\langle : J^{\hat{\alpha}} : \rangle_\beta = -\sum_{j\neq 0}\lim_{\substack{\boldsymbol{x}'\to\boldsymbol{x} \\ \Delta t\to ij\beta}} \mathcal{B}_F(s_j)\mathrm{tr}[\gamma^{\hat{\alpha}}\slashed{n}_j\Lambda_j(x_j, x')], \tag{6.13}$$

where again we have used the fact that $\Lambda(x, x) = 1$. To evaluate the above trace, we note that $\slashed{n}_j\Lambda_j(x_j, x')$ (4.16) reduces in the limit $\boldsymbol{x}' \to \boldsymbol{x}$ to:

$$\slashed{n}_j\Lambda_j(x_j, x')\rfloor_{\boldsymbol{x}'=\boldsymbol{x}} = \frac{\sin(\omega\Delta t_j/2)}{\cos\omega r\sin(\omega s_j/2)}\gamma^{\hat{0}}. \tag{6.14}$$

Inserting the result (6.14) into (6.13) and using (6.10) to eliminate the geodetic interval gives:

$$\langle : J^{\hat{\alpha}} : \rangle_{\beta} = -\eta^{\hat{\alpha}\hat{0}} \frac{\omega^3 \Gamma(2+k)(\cos \omega r)^{3+2k}}{\pi^{3/2} 4^{1+k} \Gamma(\frac{1}{2}+k)} \sum_{j\neq 0} \frac{(-1)^j \sinh \frac{\omega j \beta}{2}}{\left(\sinh^2 \frac{\omega j \beta}{2}\right)^{2+k}}$$

$$\times {}_2F_1\left(k, 2+k; 1+2k; -\frac{\cos^2 \omega r}{\sinh^2 \frac{\omega j \beta}{2}}\right), \qquad (6.15)$$

where we have also used (5.7). It can be seen that $\langle : J^{\hat{\alpha}} : \rangle_{\beta}$ vanishes, since the summand above is odd with respect to $j \to -j$.

This result is not unexpected. In [14] we found that the v.e.v. of the CC vanished when the fermion field is in the global adS vacuum. In a thermal state, we would anticipate that particle and anti-particle configurations would be equally populated, resulting in a net vanishing expectation value for the CC.

6.4. Stress-energy tensor

Before attempting to compute the difference between the t.e.v. and the v.e.v. of the SET, we use (4.14) to show that the covariant derivative of the vacuum Feynman Green's function (5.2) takes the form

$$D_{\hat{\rho}}\left[iS_F(x,x')\right] = \omega \left[\left(\frac{\partial \mathcal{A}_F}{\partial(\omega s)} + \frac{\mathcal{A}_F}{2}\tan\frac{\omega s}{2}\right)n_{\hat{\rho}} + \frac{\mathcal{A}_F}{2}\tan\left(\frac{\omega s}{2}\right)\gamma_{\hat{\rho}}\rlap{/}{n} \right.$$

$$\left. + \left(\frac{\partial \mathcal{B}_F}{\partial(\omega s)} - \frac{\mathcal{B}_F}{2}\cot\frac{\omega s}{2}\right)n_{\hat{\rho}}\rlap{/}{n} - \frac{\mathcal{B}_F}{2}\cot\left(\frac{\omega s}{2}\right)\gamma_{\hat{\rho}}\right]\Lambda(x,x'). \qquad (6.16)$$

Similarly, the derivative of $S_F(x,x')$ with respect to x' can be written as:

$$D_{\hat{\rho}'}\left[iS_F(x,x')\right] = \omega\Lambda(x,x')\left[\left(\frac{\partial \mathcal{A}_F}{\partial(\omega s)} + \frac{\mathcal{A}_F}{2}\tan\frac{\omega s}{2}\right)n_{\hat{\rho}'} + \frac{\mathcal{A}_F}{2}\tan\left(\frac{\omega s}{2}\right)\rlap{/}{n}'\gamma_{\hat{\rho}'} \right.$$

$$\left. - \left(\frac{\partial \mathcal{B}_F}{\partial(\omega s)} - \frac{\mathcal{B}_F}{2}\cot\frac{\omega s}{2}\right)\rlap{/}{n}'n_{\hat{\rho}'} + \frac{\mathcal{B}_F}{2}\cot\left(\frac{\omega s}{2}\right)\gamma_{\hat{\rho}}\right]. \qquad (6.17)$$

The results (6.16–6.17) also hold for the case when $S_F(x,x')$ is replaced by $S_F(t+ij\beta, \boldsymbol{x}; t', \boldsymbol{x}')$ and s is replaced by s_j. Using the following expressions:

$$\text{tr}[\gamma_{\hat{\alpha}}\rlap{/}{n}\Lambda(x,x')]_{\boldsymbol{x}'=\boldsymbol{x}} = -\text{tr}[\Lambda(x,x')\rlap{/}{n}'\gamma_{\hat{\alpha}'}]_{\boldsymbol{x}'=\boldsymbol{x}} = -\frac{4\sin(\omega\Delta t/2)}{\cos\omega r \sin(\omega s/2)}\delta^{\hat{0}}{}_{\hat{\alpha}}, \qquad (6.18)$$

the difference between the t.e.v. and the v.e.v. of the SET can be written as:

$$\langle : T_{\hat{\alpha}\hat{\rho}} : \rangle_{\beta} = 2i\omega\sum_{j\neq 0}(-1)^j\left[\eta_{\hat{\alpha}\hat{\rho}}\frac{\cos(\omega\Delta t_j/2)}{\sin(\omega s_j/2)}\mathcal{B}_F\right.$$

$$\left. - \frac{\sin(\omega\Delta t/2)}{\cos\omega r \sin(\omega s/2)}\left(\frac{\partial\mathcal{B}_F}{\partial(\omega s_j)} - \frac{\mathcal{B}_F}{2}\cot\frac{\omega s_j}{2}\right)\delta^{\hat{0}}{}_{(\hat{\alpha}}(n_{j\hat{\rho}}) - n_{j\hat{\rho}'})\right], \qquad (6.19)$$

where $n_{j\hat{\rho}}$ is the $\hat{\rho}$ tetrad component of the vector n_j. The primed indices in (6.19) were not parallel-transported to x, since the bivectors of parallel transport in (6.3) reduce to

Kronecker deltas when $x' = x$. The coincidence limits of $n_{j\hat\alpha}$ and $n_{j\hat\alpha'}$ are:

$$n_{j\hat0}\big|_{x'=x} = -n_{j\hat0'}\big|_{x'=x} = \frac{\cos(\omega\Delta t_j/2)}{\cos(\omega s_j/2)},$$

$$n_{j\hat\imath}\big|_{x'=x} = n_{j\hat\imath'}\big|_{x'=x} = \frac{x^i}{r}\frac{\sin(\omega\Delta t_j/2)}{\cos(\omega s_j/2)}\tan\omega r, \qquad (6.20)$$

and hence the second term in (6.19) contributes only when $\hat\alpha = \hat\rho = t$, so that $\langle : T_{\hat0\hat\imath} : \rangle_\beta = 0$.

Thus, the non-vanishing components of $\langle : T_{\hat\alpha\hat\rho} : \rangle_\beta$ are:

$$\langle : T_{\hat0\hat0} : \rangle_\beta = -2i\omega\sum_{j\neq0}(-1)^j\frac{\cos(\omega\Delta t_j/2)}{\cos(\omega s_j/2)}\frac{\partial\mathcal{B}_F(s)}{\partial(\omega s/2)}\bigg|_{s=s_j}, \qquad (6.21)$$

$$\langle : T_{\hat\imath\hat\ell} : \rangle_\beta = 2i\omega\delta_{i\ell}\sum_{j\neq0}(-1)^j\frac{\cos(\omega\Delta t_j/2)}{\sin(\omega s_j/2)}\mathcal{B}_F(s_j). \qquad (6.22)$$

The above results indicate that the difference between the t.e.v. and the v.e.v. of the SET corresponds to that of an ideal fluid [27]:

$$\langle : T^{\hat\alpha\hat\rho} : \rangle_\beta = (E_\beta + P_\beta)u^{\hat\alpha}u^{\hat\rho} + \eta^{\hat\alpha\hat\rho}P_\beta, \qquad (6.23)$$

where $E_\beta = \langle : T_{\hat0\hat0} : \rangle_\beta$ and $P_\beta = \frac{1}{3}\delta^{ij}\langle : T_{\hat\imath\hat\jmath} : \rangle_\beta$ are, respectively, the energy density and isotropic pressure at inverse temperature β, while the macroscopic velocity $u^{\hat\alpha} = (1,0,0,0)^T$ corresponds to that of a fluid at rest. Using (5.7), we find the following expressions for the energy density E_β and pressure P_β:

$$E_\beta + P_\beta = -\frac{2\omega^4\Gamma(3+k)(\cos\omega r)^{4+2k}}{\pi^{3/2}4^{1+k}\Gamma(\frac{1}{2}+k)}\sum_{j=1}^{\infty}(-1)^j\frac{\cosh\frac{\omega j\beta}{2}}{(\sinh\frac{\omega j\beta}{2})^{4+2k}}$$

$$\times {}_2F_1\left[k, 3+k; 1+2k; -\frac{\cos^2\omega r}{\sinh^2\frac{\omega j\beta}{2}}\right], \qquad (6.24)$$

$$P_\beta = -\frac{\omega^4\Gamma(2+k)(\cos\omega r)^{4+2k}}{\pi^{3/2}4^{1+k}\Gamma(\frac{1}{2}+k)}\sum_{j=1}^{\infty}(-1)^j\frac{\cosh\frac{\omega j\beta}{2}}{(\sinh\frac{\omega j\beta}{2})^{4+2k}}$$

$$\times {}_2F_1\left[k, 2+k; 1+2k; -\frac{\cos^2\omega r}{\sinh^2\frac{\omega j\beta}{2}}\right]. \qquad (6.25)$$

In the massless limit ($k = 0$), the energy density reduces to

$$E_\beta = -\frac{3\omega^4}{4\pi^2}(\cos\omega r)^4\sum_{j=1}^{\infty}(-1)^j\frac{\cosh\frac{\omega j\beta}{2}}{(\sinh\frac{\omega j\beta}{2})^4}, \qquad (6.26)$$

while $P_\beta = E_\beta/3$. Therefore, in the massless limit the trace $\langle : T_{\hat\alpha}^{\hat\alpha} : \rangle_\beta$ vanishes, as expected from (6.4), although the FC (6.12) is nonzero when the fermion is massless.

7. Kinetic theory results

In the kinetic theory approach, the dynamics of a gas of particles of momentum $p^{\hat\alpha}$ and mass m in general relativity can be described using the Boltzmann equation written

with respect to tetrad components [18, 19, 28]:

$$p^{\hat{\alpha}} e_{\hat{\alpha}}^{\mu} \frac{\partial f}{\partial x^{\mu}} - \Gamma_{\hat{\alpha}\hat{\rho}}^{\hat{i}} p^{\hat{\alpha}} p^{\hat{\rho}} \frac{\partial f}{\partial p^{\hat{i}}} = C[f] \tag{7.1}$$

where f is the particle distribution function and $C[f]$ represents the collision operator which drives the system towards equilibrium. The time component $p^{\hat{0}}$ of the particle momentum four-vector is determined from the mass-shell condition $p^{\hat{0}} = \sqrt{m^2 + \boldsymbol{p}^2}$. States in thermal equilibrium are described by the equilibrium distribution function:

$$f_{\epsilon}^{(\text{eq})}(\beta) = \frac{Z/(2\pi)^3}{e^{-\widetilde{\beta}\mu - \widetilde{\beta}p_{\hat{\alpha}} u^{\hat{\alpha}}} - \epsilon}, \tag{7.2}$$

where Z represents the number of degrees of freedom per particle and ϵ takes the values -1, 1 and 0 for Fermi-Dirac, Bose-Einstein and Maxwell-Jüttner statistics respectively. In (7.2), $\widetilde{\beta}$ represents the local inverse temperature of the state, μ is the chemical potential and $u^{\hat{\alpha}}$ is the fluid velocity four-vector. In order for the distribution function (7.2) to satisfy the Boltzmann equation (7.1), $\widetilde{\beta}\mu$ must be constant and $\widetilde{\beta}u^{\hat{\alpha}}$ must satisfy the Killing equation [29]:

$$\nabla_{\hat{\alpha}}(\widetilde{\beta}\mu) = 0, \qquad \nabla_{\hat{\alpha}}(\widetilde{\beta}u_{\hat{\sigma}}) + \nabla_{\hat{\sigma}}(\widetilde{\beta}u_{\hat{\alpha}}) = 0. \tag{7.3}$$

In this paper, we are interested in states with vanishing chemical potential $\mu = 0$, where the fluid is at rest (that is, $u^{\hat{\alpha}} = (1, 0, 0, 0)^T$). The Killing equation is satisfied with the above choice for $u^{\hat{\alpha}}$ if the inverse temperature $\widetilde{\beta}$ takes the form [16, 18]:

$$\widetilde{\beta} = \beta\sqrt{-g_{tt}} = \frac{\beta}{\cos\omega r}, \tag{7.4}$$

where $\beta \equiv \widetilde{\beta}(r = 0)$ represents the local inverse temperature at the coordinate origin. The kinetic theory formulation gives the macroscopic SET $T^{\hat{\alpha}\hat{\rho}}$ as the second order moment of the distribution function f:

$$T^{\hat{\alpha}\hat{\sigma}} = \int \frac{d^3p}{p^{\hat{0}}} f \, p^{\hat{\alpha}} p^{\hat{\sigma}}, \tag{7.5}$$

where the integration measure $d^3p/p^{\hat{0}}$ is Lorentz-invariant.

The SET corresponding to the distribution (7.2) can be found by first performing a series expansion of the equilibrium distribution function (7.2) in powers of ϵ [18, 19, 20]:

$$f_{\epsilon}^{(\text{eq})}(\beta) = \sum_{j=0}^{\infty} \epsilon^j f_0^{(\text{eq})}(\beta[j+1]), \tag{7.6}$$

where the Maxwell-Jüttner equilibrium distribution function (7.2) takes the simple form [18]

$$f_0^{(\text{eq})}(\beta) = \frac{Z}{(2\pi)^3} e^{-\beta p^{\hat{0}}}. \tag{7.7}$$

The energy density and pressure arising from the Maxwell-Jüttner distribution function (7.7) can be found in closed form [18, 19, 29]:

$$E_0(\widetilde{\beta}) - 3P_0(\widetilde{\beta}) = \frac{Zm^3 \cos\omega r}{2\pi^2\beta} K_1\left(\frac{m\beta}{\cos\omega r}\right), \tag{7.8}$$

$$P_0(\widetilde{\beta}) = \frac{Zm^2}{2\pi^2\beta^2}(\cos\omega r)^2 K_2\left(\frac{m\beta}{\cos\omega r}\right), \tag{7.9}$$

where $K_n(z)$ is a modified Bessel function of the third kind and m is the particle mass. The SET arising from the distribution (7.6) with general statistics can then be written as [27, 29]:

$$T_\epsilon^{\hat\alpha\hat\rho}(\widetilde\beta) = \left[E_\epsilon(\widetilde\beta) + P_\epsilon(\widetilde\beta)\right] u^{\hat\alpha} u^{\hat\rho} + \eta^{\hat\alpha\hat\rho} P_\epsilon(\widetilde\beta), \tag{7.10}$$

where [18, 19, 20]

$$E_\epsilon(\widetilde\beta) = \sum_{j=0}^\infty \epsilon^j E_0([j+1]\widetilde\beta), \qquad P_\epsilon(\widetilde\beta) = \sum_{j=0}^\infty \epsilon^j P_0([j+1]\widetilde\beta). \tag{7.11}$$

For thermal states of fermions ($\epsilon = -1$), the energy density and pressure (7.11) take the form [19, 20]:

$$E_{-1}(\widetilde\beta) - 3P_{-1}(\widetilde\beta) = -\frac{2m^3 \cos\omega r}{\pi^2\beta} \sum_{j=1}^\infty \frac{(-1)^j}{j} K_1\left(\frac{mj\beta}{\cos\omega r}\right), \tag{7.12}$$

$$P_{-1}(\widetilde\beta) = -\frac{2m^2}{\pi^2\beta^2}(\cos\omega r)^2 \sum_{j=1}^\infty \frac{(-1)^j}{j^2} K_2\left(\frac{mj\beta}{\cos\omega r}\right), \tag{7.13}$$

where $Z = 4$ was taken to account for the spin and charge degrees of freedom of the Dirac fermions. The FC in kinetic theory is defined analogously to (6.4):

$$FC_{-1}(\widetilde\beta) = \frac{1}{m}\left[E_{-1}(\widetilde\beta) - 3P_{-1}(\widetilde\beta)\right] = -\frac{2m^2 \cos\omega r}{\pi^2\beta} \sum_{j=1}^\infty \frac{(-1)^j}{j} K_1\left(\frac{mj\beta}{\cos\omega r}\right). \tag{7.14}$$

If we set $\omega = 0$ (so that the adS radius of curvature is infinite) in (7.12–7.14), we recover the Minkowski space-time kinetic theory quantities

$$E_{-1}(\widetilde\beta) - 3P_{-1}(\widetilde\beta)\Big|_{\omega=0} = -\frac{2m^3}{\pi^2\beta} \sum_{j=1}^\infty \frac{(-1)^j}{j} K_1\left(mj\beta\right),$$

$$P_{-1}(\widetilde\beta)\Big|_{\omega=0} = -\frac{2m^2}{\pi^2\beta^2} \sum_{j=1}^\infty \frac{(-1)^j}{j^2} K_2\left(mj\beta\right),$$

$$FC_{-1}(\widetilde\beta)\Big|_{\omega=0} = -\frac{2m^2}{\pi^2\beta} \sum_{j=1}^\infty \frac{(-1)^j}{j} K_1\left(mj\beta\right), \tag{7.15}$$

for a thermal distribution of fermions of mass m. On Minkowski space-time, the kinetic theory results (7.15) are identical to the t.e.v.s obtained using QFT (calculated in, for example, [30]). On adS space-time, the kinetic theory results corresponding to (7.11) for massless bosons ($\epsilon = 1$) do not agree with the difference between the QFT t.e.v.s and v.e.v.s computed in [8] for a massless, conformally coupled scalar field. In particular, the kinetic theory results can only depend on the inverse temperature β at the origin and the radial coordinate r as functions of the local temperature $\widetilde\beta$ (7.4). However, the QFT results in [8] have a much more complicated dependence on β and the radial coordinate r. How the kinetic theory results (7.12–7.14) on adS space-time compare with the QFT t.e.v.s calculated in section 6 will be the focus of section 8.

In the massless limit ($m = 0$), using the asymptotic behaviour of the Bessel functions for fixed order $\nu > 0$ as the argument z tends to zero [31]

$$K_\nu(z) \simeq \frac{1}{2}\Gamma(\nu)\left(\frac{1}{2}z\right)^{-\nu}, \qquad z \to 0, \tag{7.16}$$

the kinetic theory energy density (7.12) reduces to:

$$E_{-1}(\widetilde{\beta})\rfloor_{m=0} = \frac{12}{\pi^2\beta^4}(\cos\omega r)^4\sum_{j=1}^\infty \frac{(-1)^{j+1}}{j^4} = \frac{7\pi^2}{60\beta^4}(\cos\omega r)^4, \tag{7.17}$$

while $P_{-1}(\widetilde{\beta})\rfloor_{m=0} = \frac{1}{3}E_{-1}(\widetilde{\beta})\rfloor_{m=0}$. We note that the kinetic theory FC (7.14) vanishes in the massless limit, $FC_{-1}(\widetilde{\beta}) = 0$ when $m = 0$, in contrast to the nonzero expression (6.12) for the QFT FC_β for massless fermions. This is our first indication that quantum corrections are significant for t.e.v.s for fermions on adS.

8. Comparing the QFT and kinetic theory results

We now compare our QFT results obtained in section 6 with the kinetic theory results from section 7, both analytically and numerically. We begin in subsection 8.1 by comparing the profiles of the FC, energy density, pressure and equation of state $w = P/E$. Next, subsection 8.2 discusses their behaviour in the vicinity of the adS boundary and subsection 8.3 analyses these quantities at the origin. We focus on the massless case in subsection 8.4.

8.1. Profiles of the FC, energy density, pressure and equation of state

Figure 1 shows the profiles of the FC, energy density E, pressure P and equation of state $w = P/E$ as derived in QFT (dashed lines) and kinetic theory (solid lines) as functions of the radial coordinate ωr, for two different values of the inverse temperature: $\beta\omega = 0.5$ (left) and $\beta\omega = 2.0$ (right) and various values of the fermion mass $m = k\omega$.

For the FC, we compare the QFT result (6.11) with that arising from kinetic theory (7.14) in figure 1(a–b). In both formulations, the profiles of the FC have similar qualitative features for all values of the inverse temperature and fermion mass studied in figure 1. In particular, there is a maximum at the origin and both the energy density and pressure tend to zero as $\omega r \to \pi/2$ and the space-time boundary is approached. This arises from the overall powers of $\cos\omega r$ in (6.11, 7.14). Thermal radiation is concentrated near the origin, away from the space-time boundary. This can also be understood from the Tolman relation (7.4) for the local temperature $\widetilde{\beta}^{-1}$ which has a maximum at the origin and vanishes on the boundary. It is also clear from figure 1 that considering a thermal state has broken the space-time symmetries and the t.e.v.s are not constant throughout the space-time, unlike the v.e.v.s computed in [14]. The kinetic theory FC (7.14) vanishes when $k = 0$ and the fermion field is massless. We see from figure 1(a–b) that the QFT result (6.12), while nonzero, is very small, even when $\beta\omega = 0.5$ and the temperature is large.
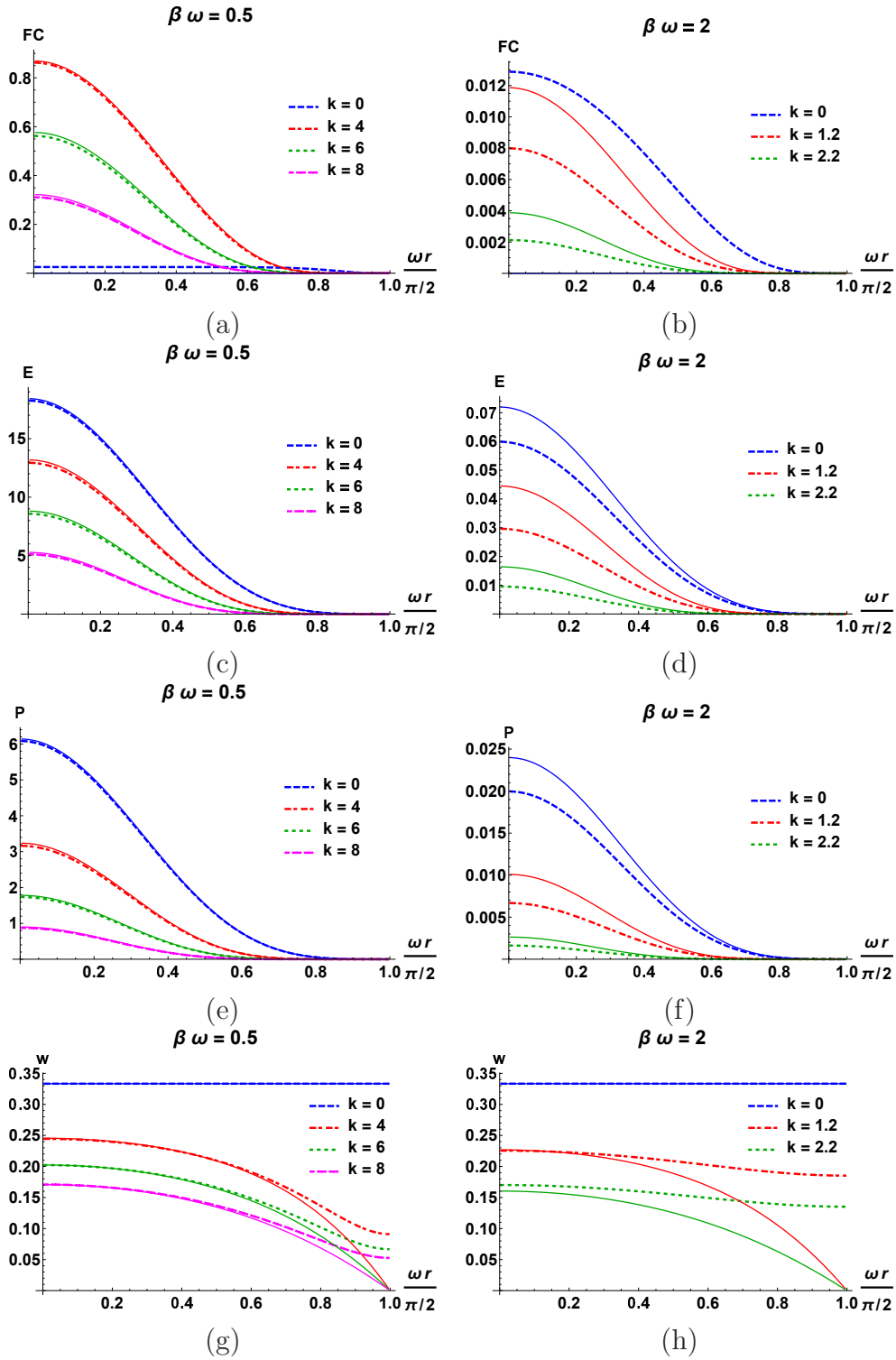
Figure 1. Comparison between the QFT (dashed lines) and kinetic theory (continuous lines) results for the profiles of the FC (top line), energy density E (second line), pressure P (third line) and equation of state $w = P/E$ (bottom line), for $\beta\omega = 0.5$ (left) and $\beta\omega = 2.0$ (right). The curves correspond to various values of $k = m/\omega$.

Looking at figure 1(c–f), the profiles of energy density and pressure in both QFT and kinetic theory have similar qualitative features to the profiles of the FC for all values of the inverse temperature and fermion mass studied. The overall factors of powers of $\cos(\omega r)$ appearing in (6.24, 6.25, 7.12, 7.13) mean that the profiles have a maximum at the origin and tend to zero on the space-time boundary.

In general, quantum effects (that is, deviations from classical kinetic theory) will occur in the presence of strong gravitational fields, where the coupling between the space-time curvature and the quantum fields becomes important. On adS, the space-time curvature is proportional to the inverse radius of curvature ω. We anticipate that at low values of $\beta\omega$ (corresponding to large temperatures) the QFT results derived in section 6 should approach the kinetic theory results from section 7. As $\beta\omega$ increases, and the temperature decreases, we expect to see deviations from kinetic theory in the QFT results. These expectations are confirmed in figure 1(a–f), where it can be seen that when $\beta\omega = 0.5$, the profiles obtained using QFT and kinetic theory are nearly indistinguishable, and visible deviations between these two approaches appear when $\beta\omega = 2.0$.

Figure 1(g–h) show the profiles of the equation of state $w = P/E$ as a function of ωr. As expected from sections 6 and 7, the equation of state equals one third for all ωr when the fermion field is massless ($k = 0$). However, for a massive fermion field, figure 1 reveals fundamental differences between QFT and kinetic theory in the properties of the equation of state. In the framework of kinetic theory, the equation of state $w_{-1}(\widetilde{\beta}) = P_{-1}(\widetilde{\beta})/E_{-1}(\widetilde{\beta})$ always approaches 0 as $\omega r \to \pi/2$ as long as $k = m/\omega > 0$. This is in contrast with the QFT results, which show a temperature-independent nonzero value of the equation of state $w_\beta = P_\beta/E_\beta$ on the adS boundary. To understand this behaviour in more detail, in the following subsection we examine more closely the FC, energy density, pressure and equation of state in the vicinity of the boundary.

8.2. Behaviour near the boundary

Near the boundary, it is useful to change the radial variable from ωr to δ, where

$$\delta = \frac{\pi}{2} - \omega r, \tag{8.1}$$

with $\cos\omega r = \sin\delta$. For small values of the argument, the hypergeometric functions appearing in (6.11, 6.24, 6.25) have the series expansion [31]:

$$_2F_1(a, b; c; z) = 1 + \frac{ab}{c}z + O(z^2). \tag{8.2}$$

Thus, the QFT t.e.v.s of the FC, energy density and pressure (6.11, 6.24, 6.25) can be approximated by the following expressions:

$$FC_\beta \simeq \frac{2\omega^3\Gamma(2+k)(\sin\delta)^{4+2k}}{\pi^{3/2}4^{1+k}\Gamma(\frac{1}{2}+k)}\left[S_k - \frac{(1+k)(2+k)}{1+2k}S_{1+k}\sin^2\delta\right], \tag{8.3}$$

$$E_\beta \simeq \frac{\omega^4\Gamma(2+k)(\sin\delta)^{4+2k}}{\pi^{3/2}4^{1+k}\Gamma(\frac{1}{2}+k)}\left[(3+2k)S_k - \frac{k(2+k)}{1+2k}(5+2k)S_{1+k}\sin^2\delta\right], \tag{8.4}$$

$$P_\beta \simeq \frac{\omega^4 \Gamma(2+k)(\sin\delta)^{4+2k}}{\pi^{3/2}4^{1+k}\Gamma(\frac{1}{2}+k)}\left[S_k - \frac{k(2+k)}{1+2k}S_{1+k}\sin^2\delta\right], \tag{8.5}$$

where we have retained terms up to and including corrections of second order in $\sin\delta$ and

$$S_\nu = -\sum_{j=1}^{\infty}(-1)^j \frac{\cosh\frac{\omega j\beta}{2}}{(\sinh\frac{\omega j\beta}{2})^{4+2\nu}}. \tag{8.6}$$

It can be seen that the QFT t.e.v.s of FC_β, the energy density E_β and pressure P_β all approach 0 as $(\sin\delta)^{4+2k}$ for $\delta \to 0$. For small δ, the equation of state from QFT can be approximated by the expression:

$$w_\beta = \frac{P_\beta}{E_\beta} \simeq \left[3+2k - \frac{2k(2+k)}{1+2k}\frac{S_{k+1}}{S_k}\sin^2\delta\right]^{-1}. \tag{8.7}$$

As $\delta \to 0$, the equation of state $w_\beta \to (3+2k)^{-1}$, which is confirmed by the numerical results presented in figure 1(g–h).

In order to find the behaviour near the boundary of the energy density (7.12), pressure (7.13) and FC (7.14) obtained using kinetic theory, the following asymptotic expression for the modified Bessel functions $K_\nu(z)$ when the argument is large can be employed [31]:

$$K_\nu(z) = \sqrt{\frac{\pi}{2z}}e^{-z}\left[1 + \frac{4\nu^2-1}{8z} + O(z^{-2})\right], \qquad z\to\infty. \tag{8.8}$$

In the following we assume that the fermion mass $m > 0$. We first consider the expansion for $P_{-1}(\widetilde{\beta})$ (7.13):

$$P_{-1}(\widetilde{\beta}) \simeq -\frac{1}{2}\left(\frac{2m}{\pi}\right)^{3/2}\left(\frac{\sin\delta}{\beta}\right)^{5/2}\sum_{j=1}^{\infty}\frac{(-1)^j}{j^{5/2}}e^{-mj\beta/\sin\delta}\left[1 + \frac{15\sin\delta}{8mj\beta} + O(\delta^2)\right]. \tag{8.9}$$

Due to the exponential decrease of the summand, a suitable approximation can be obtained by truncating the sum over j after the first term, yielding:

$$P_{-1}(\widetilde{\beta}) \simeq \frac{1}{2}\left(\frac{2m}{\pi}\right)^{3/2}\left(\frac{\sin\delta}{\beta}\right)^{5/2}e^{-m\beta/\sin\delta}\left(1 + \frac{15}{8m\beta}\sin\delta\right). \tag{8.10}$$

The difference $E_{-1}(\widetilde{\beta}) - 3P_{-1}(\widetilde{\beta})$ can be similarly approximated from (7.12):

$$E_{-1}(\widetilde{\beta}) - 3P_{-1}(\widetilde{\beta}) \simeq \frac{m}{2}\left(\frac{2m}{\pi}\right)^{3/2}\left(\frac{\sin\delta}{\beta}\right)^{3/2}e^{-m\beta/\sin\delta}\left(1 + \frac{3}{8m\beta}\sin\delta\right). \tag{8.11}$$

We then also have an approximation for the FC in kinetic theory from (7.14):

$$FC_{-1}(\widetilde{\beta}) \simeq \frac{1}{2}\left(\frac{2m}{\pi}\right)^{3/2}\left(\frac{\sin\delta}{\beta}\right)^{3/2}e^{-m\beta/\sin\delta}\left(1 + \frac{3}{8m\beta}\sin\delta\right). \tag{8.12}$$

Since the power of $\sin\delta$ in (8.11) is smaller than that in (8.10), the energy density dominates over the pressure as the boundary is approached. This can be seen by considering the behaviour of the equation of state:

$$w_{-1}(\widetilde{\beta}) = \frac{P_{-1}(\widetilde{\beta})}{E_{-1}(\widetilde{\beta})} \simeq \sin\delta\left(m\beta + \frac{3}{2}\sin\delta\right)^{-1}. \tag{8.13}$$

As $\delta \to 0$, the equation of state in kinetic theory tends to 0 as the boundary is approached, providing the fermion mass $m > 0$, as is confirmed in figure 1(g–h). Our approximations near the boundary for the kinetic theory results are not valid if the fermion is massless $m = 0$, when the energy density takes the simple form (7.17) and the equation of state equals one third everywhere.

In figure 2 we compare our analytic approximations near the space-time boundary with the full numerical t.e.v.s derived in both QFT (left) and kinetic theory (right), for inverse temperature $\beta\omega = 1$. In order to maximise the visibility of the domain of applicability of our results, the ratio between the FC, energy density and pressure and their leading order asymptotic behaviour (8.3–8.5, 8.10–8.12) is taken, in other words we plot the following quantities:

$$FC^{\text{reg}}_{\beta} = \frac{FC_{\beta}}{(\cos\omega r)^{4+2k}}, \quad E^{\text{reg}}_{\beta} = \frac{E_{\beta}}{(\cos\omega r)^{4+2k}}, \quad P^{\text{reg}}_{\beta} = \frac{P_{\beta}}{(\cos\omega r)^{4+2k}},$$

$$FC^{\text{reg}}_{-1}(\widetilde{\beta}) = \frac{FC_{-1}(\widetilde{\beta})}{e^{-m\beta/\cos\omega r}(\cos\omega r)^{3/2}}, \quad E^{\text{reg}}_{-1}(\widetilde{\beta}) = \frac{E_{-1}(\widetilde{\beta})}{e^{-m\beta/\cos\omega r}(\cos\omega r)^{3/2}},$$

$$P^{\text{reg}}_{-1}(\widetilde{\beta}) = \frac{P_{-1}(\widetilde{\beta})}{e^{-m\beta/\cos\omega r}(\cos\omega r)^{5/2}}, \tag{8.14}$$

where the QFT quantities FC_{β}, the energy density E_{β} and pressure P_{β} are given by (6.11, 6.24, 6.25) and the kinetic theory energy density $E_{-1}(\widetilde{\beta})$, pressure $P_{-1}(\widetilde{\beta})$ and $FC_{-1}(\widetilde{\beta})$ by (7.12, 7.13, 7.14). We also plot the equations of state for QFT and kinetic theory, given respectively by

$$w_{\beta} = \frac{P_{\beta}}{E_{\beta}} = \frac{P^{\text{reg}}_{\beta}}{E^{\text{reg}}_{\beta}}, \qquad w_{-1}(\widetilde{\beta}) = \frac{P_{-1}(\widetilde{\beta})}{E_{-1}(\widetilde{\beta})} = \frac{P^{\text{reg}}_{-1}(\widetilde{\beta})\cos\omega r}{E^{\text{reg}}_{-1}(\widetilde{\beta})}. \tag{8.15}$$

For both QFT and kinetic theory, in figure 2 our approximations can be seen to hold in a vicinity of the boundary. In the kinetic theory case (right-hand plots in figure 2) the analytic expressions (8.10, 8.11, 8.12) for $FC_{-1}(\widetilde{\beta})$, the energy density $E_{-1}(\widetilde{\beta})$ and pressure $P_{-1}(\widetilde{\beta})$ are good approximations to the exact results (7.12, 7.13, 7.14) everywhere in the space-time and for all values of the fermion mass shown, although the resulting approximation (8.13) for the equation of state $w_{-1}(\widetilde{\beta})$ is not very accurate away from the boundary when k is small. In the QFT case (left-hand plots in figure 2), the analytic expressions (8.3–8.5) for FC_{β}, the energy density E_{β} and pressure P_{β} are good approximations to the exact results (6.11, 6.24, 6.25) in only a small neighbourhood of the boundary.

The analysis presented in this subsection points to a fundamental difference between the kinetic theory and QFT approaches. While in the kinetic theory formulation, the equation of state on the space-time boundary can only have two values (namely 1/3 for massless particles and 0 for any nonzero mass), the QFT results allow w to undertake a slow, temperature-independent transition from 1/3 for massless fermions down to 0 as $k = m/\omega$ tends to large values.
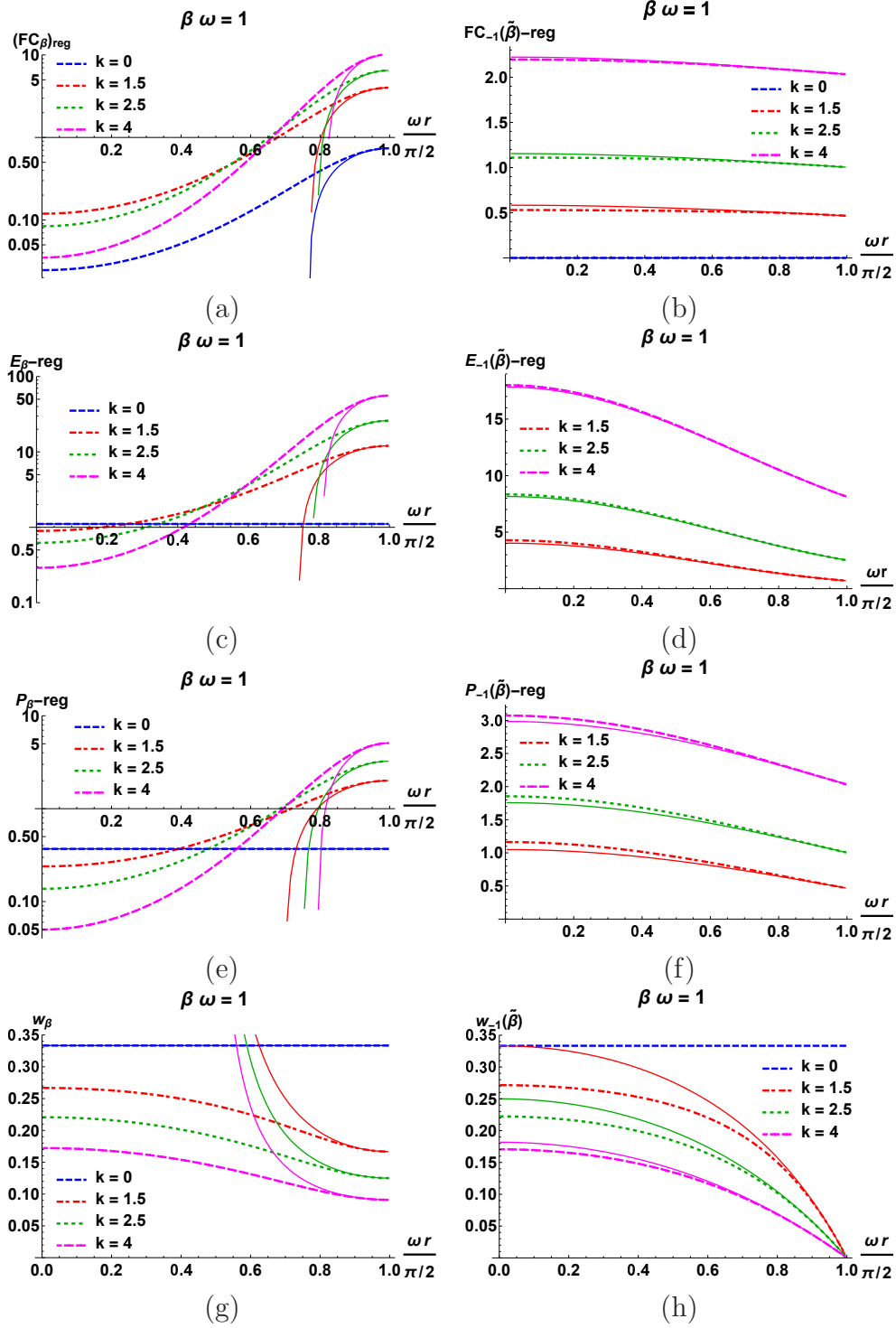
Figure 2. Comparison between the exact numerical profiles of the FC (top line), energy density E (second line), pressure P (third line) and equation of state $w = P/E$ (bottom line) and the asymptotic formulae presented in section 8.2. The QFT results are shown in the left column, while the kinetic theory results are presented in the right column. In each case, the continuous lines correspond to the asymptotic approximations, while the dashed lines are the exact QFT/kinetic theory results.
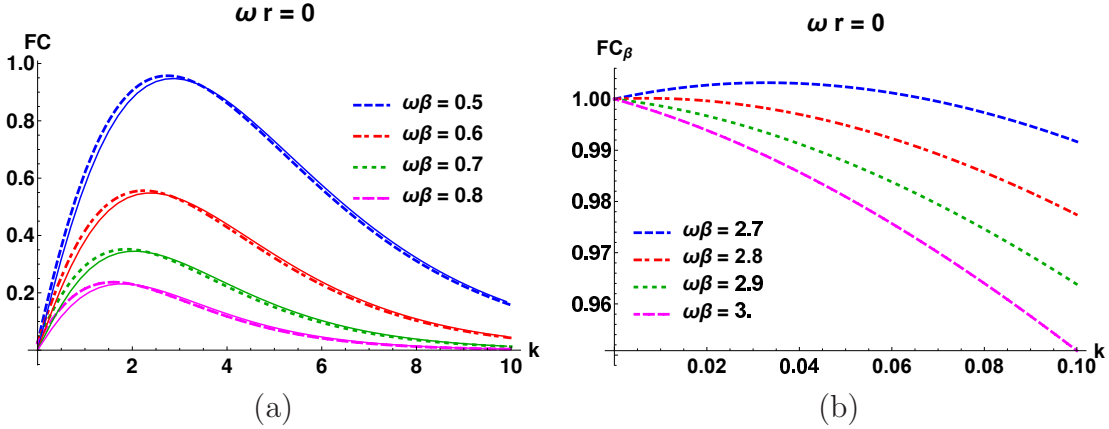
Figure 3. (a) FC_β (6.11) (dashed lines) and $FC_{-1}(\widetilde{\beta})$ (7.14) (continuous lines) evaluated at the origin $\omega r = 0$ as functions of $k = m/\omega$ for various values of the inverse temperature β. (b) FC_β (6.11) for a massive fermion field at the origin divided by FC_β for a massless fermion field at the origin, again as a function of k for various values of $\beta\omega$.

8.3. Behaviour at the origin

We have seen from the profiles in figure 1 that the FC, energy density and pressure all take their maximum values at the origin for fixed inverse temperature β and fermion mass m. To explore in more detail how the results from both QFT and kinetic theory depend on the fermion mass and temperature, in this section we consider the behaviour of all quantities at the space-time origin. The maximal symmetry of adS is broken by fixing the inverse temperature at the point selected to be the origin, and the local inverse temperature (7.4) is then defined relative to the inverse temperature at the origin.

We begin by considering FC_β (6.11) and $FC_{-1}(\widetilde{\beta})$ (7.14) evaluated at the origin in figure 3. In the left-hand plot we show the values at the origin in both QFT and kinetic theory as a function of $k = m/\omega$ for a selection of values of the inverse temperature $\beta\omega$. For fixed temperature, the QFT FC_β at the origin is very small (but nonzero) when the fermion field is massless ($k = 0$), whereas the kinetic theory $FC_{-1}(\widetilde{\beta})$ vanishes when $k = 0$. As k increases with β fixed for the values of $\beta\omega$ in figure 3(a), both FC_β and $FC_{-1}(\widetilde{\beta})$ at the origin increase until they reach a maximum at a certain value of the fermion mass. They then decrease monotonically as k increases for these values of β.

At the origin, the kinetic theory quantity $FC_{-1}(\widetilde{\beta})$ (7.14) has the same value as it does in Minkowski space-time (7.15). Therefore the qualitative shape of the profile of $FC_{-1}(\widetilde{\beta})$ as a function of $k = m/\omega$ does not change as β varies and for all β there is a maximum at some value of k. In contrast, for the QFT quantity FC_β considered at the origin as a function of k, the behaviour shown in figure 3(a) at comparatively small values of $\beta\omega$ (corresponding to high temperatures) does not persist for larger values of $\beta\omega$. This can be seen in figure 3(b), where we show the FC_β at the origin for nonzero k divided by FC_β at the origin when $k = 0$ for a selection of larger values of $\beta\omega$. We divide
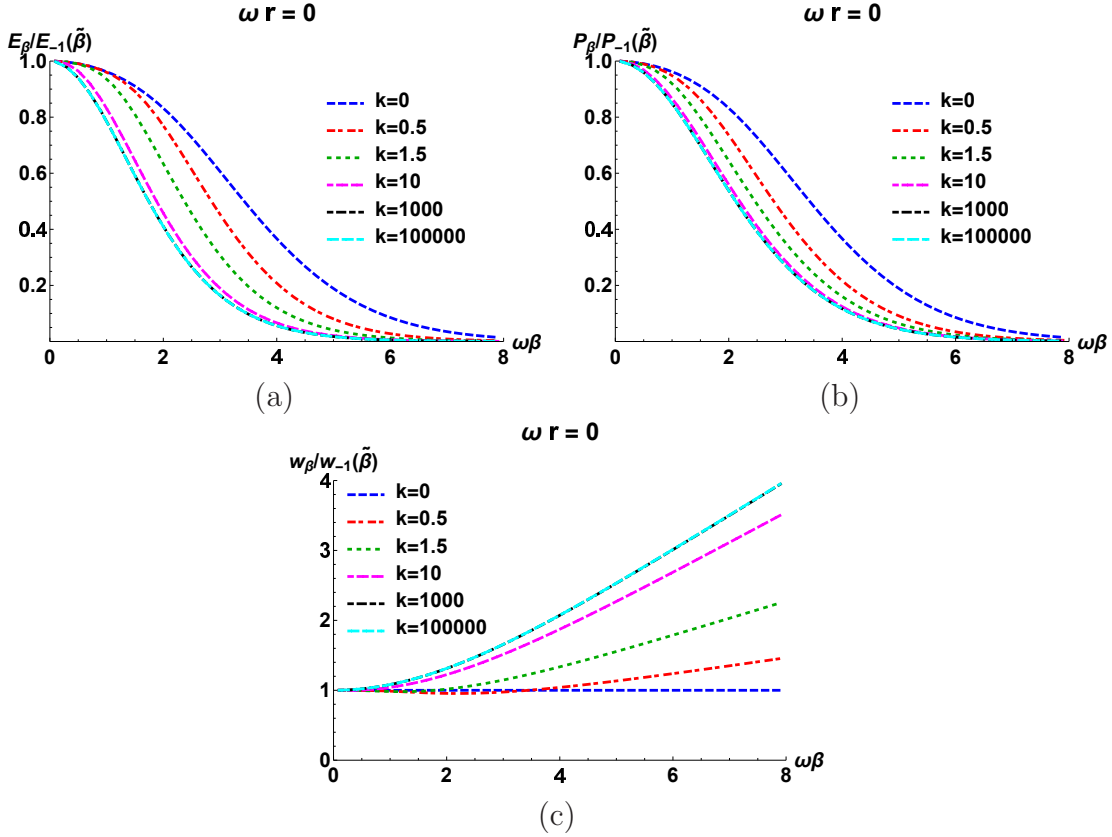
Figure 4. (a) The ratio $E_\beta/E_{-1}(\widetilde{\beta})$ between the energy densities obtained using QFT (6.24) and kinetic theory (7.12), (b) the ratio $P_\beta/P_{-1}(\widetilde{\beta})$ between the pressures obtained from QFT (6.25) and kinetic theory (7.13), (c) the ratio $w_\beta/w_{-1}(\widetilde{\beta})$ between the equations of state corresponding to QFT and kinetic theory. All quantities are plotted as functions of $\beta\omega$ for a selection of fixed values of $k = m/\omega$.

by the FC at the origin for $k = 0$ in figure 3(b) to make the behaviour easier to see. When $\beta\omega = 2.7$, we see that FC_β at the origin initially increases for increasing k, reaches a maximum and then decreases as k increases further. However, for $\beta\omega \geq 2.82857$, we find that FC_β is monotonically decreasing as k increases from zero. In order to find this value of $\beta\omega$ where FC_β no longer initially increases with k, we compute the following derivative:

$$\frac{d(FC_\beta)}{dk}\bigg|_{k=0,\omega r=0} = -\frac{\omega^3}{2\pi^2}\sum_{j=1}^{\infty}(-1)^j\left(\frac{1}{\cosh\frac{\omega j\beta}{2}\sinh^2\frac{\omega j\beta}{2}} - \frac{\ln\left[\sinh^2\frac{\omega j\beta}{2}\right]}{\cosh^3\frac{\omega j\beta}{2}}\right). \qquad (8.16)$$

The value of $\beta\omega$ where the above derivative vanishes is found numerically to be ~ 2.82857, which is close, but not equal to $\sqrt{8} \simeq 2.82843$.

For the energy density and pressure, in both QFT and kinetic theory, we find a much simpler dependence on k and $\beta\omega$ at the origin; as either k increases or $\beta\omega$ increases, the values at the origin decrease. We examine how the QFT and kinetic theory results compare in figure 4. At finite values of k, figure 4(a) shows that the ratio between the QFT result for the energy density (6.24) and the kinetic theory energy density (7.12)

decreases as k increases for fixed values of $\omega\beta$, approaching an asymptotic value as $k \to \infty$. As $\beta\omega \to 0$ and the temperature increases to infinity, the ratio $E_\beta/E_{-1}(\widetilde{\beta})$ approaches unity for all values of k examined. This is to be expected since as the temperature increases, particles of finite mass eventually behave as though they were massless. Furthermore, at large values of the temperature, the quantum corrections to the energy density are negligible and the system becomes effectively classical.

Figure 4(b) presents a similar plot for the ratio between the QFT pressure (6.25) and the kinetic theory pressure (7.13). It can be seen that the asymptotic behaviour is approached at a smaller value of k, while $P_\beta/P_{-1}(\widetilde{\beta})$ decreases more slowly with $\omega\beta$ than the energy density ratio presented in figure 4(a).

Finally, the equation of state $w_\beta = P_\beta/E_\beta$ is shown in figure 4(c), divided by the equation of state $w_{-1}(\widetilde{\beta}) = P_{-1}(\widetilde{\beta})/E_{-1}(\widetilde{\beta})$ predicted by kinetic theory. It can be seen that, for large enough values of $\beta\omega$, the ratio $w_\beta/w_{-1}(\widetilde{\beta})$ increases as $\beta\omega$ increases, approaching an asymptotic value as $k \to \infty$. These results indicate that the energy density is more strongly quenched by quantum corrections than the pressure.

8.4. Massless limit

We close this section by further examining the effect of quantum corrections on the energy density, restricting our attention to the massless limit $k = 0$, when the pressure is always one third of the energy density in both QFT and kinetic theory. The expressions for the energy density obtained using QFT (6.26) and kinetic theory (7.17) simplify considerably for massless fermions, which aids our analysis. In both the QFT (6.26) and kinetic theory (7.17) energy densities, the coordinate dependence is contained only in an overall factor of $(\cos \omega r)^4$. To see the effect of quantum corrections, it is instructive to consider the low- and high-temperature approximations to the QFT energy density (6.26).

To examine the high-temperature limit, we consider an expansion of (6.26) in powers of $\beta\omega \ll 1$:

$$E_\beta = \frac{7\pi^2}{60\beta^4}(\cos \omega r)^4 \left[1 - \frac{5\beta^2\omega^2}{14\pi^2} - \frac{17\beta^4\omega^4}{112\pi^4} + O([\beta\omega]^6) \right]. \tag{8.17}$$

The first term in (8.17) coincides with the kinetic theory result in (7.17), while the second and third terms represent quantum corrections which go to 0 as $\beta\omega \to 0$.

The large $\beta\omega$ (low-temperature) behaviour of (6.26) can be investigated by considering the following series [30]:

$$\frac{\cosh \frac{j\omega\beta}{2}}{(\sinh \frac{j\omega\beta}{2})^4} = 8e^{-\frac{3}{2}j\omega\beta} \sum_{n=0}^{\infty} \left(1 + \frac{13n}{6} + \frac{3n^2}{2} + \frac{n^3}{3} \right) e^{-nj\omega\beta}. \tag{8.18}$$

Substituting (8.18) into (6.26) gives an alternative formula for the QFT energy density:

$$E_\beta = -\frac{6\omega^4}{\pi^2} \frac{(\cos \omega r)^4}{1 + e^{\frac{3}{2}\omega\beta}} \sum_{n=0}^{\infty} e^{-n\omega\beta} \left(1 + \frac{13n}{6} + \frac{3n^2}{2} + \frac{n^3}{3} \right) \frac{1 + e^{-\frac{3}{2}\omega\beta}}{1 + e^{-(\frac{3}{2}+n)\omega\beta}}. \tag{8.19}$$
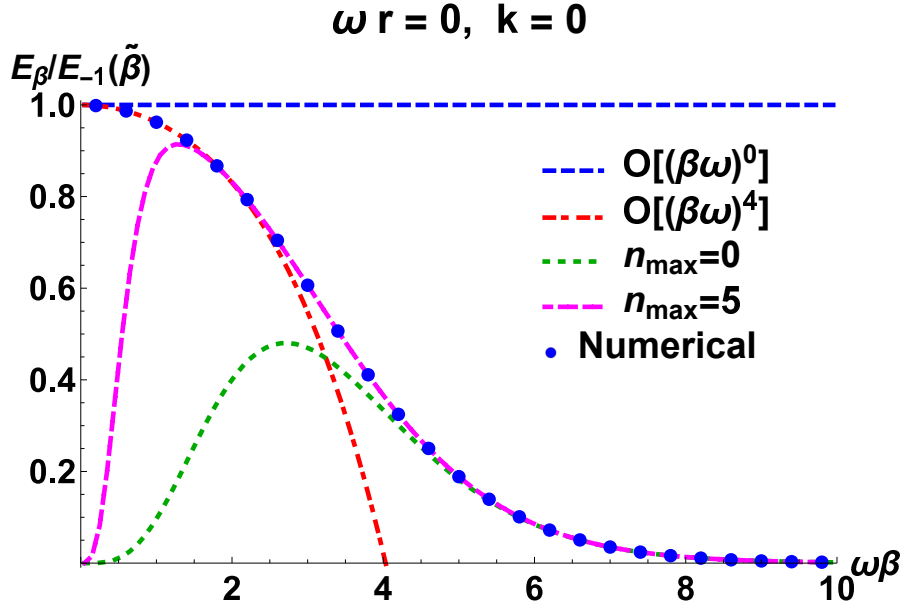
Figure 5. The effect of quantum corrections on the energy density. Blue dots show the QFT energy density E_β computed numerically from (6.26) divided by the kinetic theory result $E_{-1}(\widetilde{\beta})$ (7.17), evaluated at the origin $\omega r = 0$ as a function of $\beta\omega$ for massless fermions $k = 0$. We also plot the low- and high-temperature approximations to E_β divided by $E_{-1}(\widetilde{\beta})$. For the blue line we use the leading order $O([\beta\omega]^0)$ term in the high-temperature approximation (8.17) to E_β and for the red curve the high-temperature approximation (8.17) up to and including terms of $O([\beta\omega]^4)$. The green and pink curves are, respectively, plotted using the low-temperature expression (8.19) for the QFT energy density E_β, with only the first ($n = 0$) term in the series included for the green curve, while terms up to and including $n = 5$ are included for the pink curve.

It is clear that this tends to zero exponentially quickly as $\beta\omega \to \infty$, in contrast to the kinetic theory result (7.17) which tends to zero like $(\beta\omega)^{-4}$ as $\beta\omega \to \infty$. Thus, for low temperatures, the QFT energy density is considerably smaller than that arising from kinetic theory and quantum corrections are significant.

The effect of quantum corrections on the energy density can be seen in figure 5, where the blue dots show the QFT energy density E_β (6.26) divided by the kinetic theory energy density $E_{-1}(\widetilde{\beta})$ (7.17). As $\beta\omega \to 0$, this ratio tends to unity, as expected from (8.17), and quantum corrections are negligible. For large values of $\beta\omega$, it can be seen that the quantum corrections are significant, with the QFT energy density being many times smaller than the kinetic theory result.

In figure 5 we also show low- and high-temperature approximations to the QFT energy density E_β, again dividing by the kinetic energy density $E_{-1}(\widetilde{\beta})$. As expected, the high-temperature approximation (8.17) to E_β works well when $\beta\omega$ is small (especially the red curve, in which we retain terms up to and including $O([\beta\omega]^4)$ in (8.17)), while the first few terms in the series in (8.19) are a good approximation for the low-temperature regime (particularly the pink curve for which we use terms up to and including $n = 5$ in

the series). There is also a neighbourhood of $\beta\omega \sim 2$ where both the low-temperature series (8.19) including terms up to $n = 5$ and the high-temperature approximation (8.17) with terms up to $O([\beta\omega]^4)$ are good approximations to the QFT energy density.

9. Conclusions

In this paper we have studied t.e.v.s for a massive quantum fermion field propagating on four-dimensional adS space-time. The maximal symmetry of the space-time enables us to derive a closed-form expression for the bispinor of parallel transport, which, when combined with the imaginary time anti-periodicity property of the Feynman Green's function at finite temperature, yields expressions for the differences between the t.e.v.s and the v.e.v.s as infinite sums involving hypergeometric functions. We have also computed the corresponding quantities within relativistic kinetic theory and compared the results with the QFT expectation values. In Minkowski space-time, relativistic kinetic theory results for fermions are exactly equal to the corresponding t.e.v.s computed in QFT. We have found that this is not the case in adS space-time, and quantum corrections to the kinetic theory results are significant.

De Sitter (dS) space-time is also maximally symmetric, but has positive rather than negative cosmological constant. Due to the presence of a cosmological horizon, there is a preferred temperature for thermal states on dS space-time, namely the Gibbons-Hawking temperature [32]. For a thermal state at the Gibbons-Hawking temperature, the t.e.v. of the SET is proportional to the metric tensor and given exactly by the Brown-Ottewill-Page approximation [33].

In contrast, for adS space-time there is no such preferred temperature. Any nonzero temperature breaks the maximal symmetry of the space-time by singling out an origin at which the local inverse temperature is β. Thus, while for a massive quantum fermion field, the v.e.v. of the FC is constant everywhere in adS, and that of the SET is proportional to the metric tensor [14], the t.e.v. of the FC is not constant and that of the SET is not proportional to the metric tensor. Similar behaviour has been found in [8] for thermal states for a massless, conformally coupled, scalar field on adS. On the other hand, for all values of the fermion mass m we find that the difference between the t.e.v. and the v.e.v. of the SET has the form of an ideal fluid throughout the space-time (6.23), whereas this is not the case for the massless, conformally coupled scalar field [8].

In the massless case, the expressions (6.12, 6.26) for the t.e.v.s of the FC and energy density are rather simpler than the corresponding expressions in [8] for the t.e.v.s of the vacuum polarization and SET for a massless, conformally coupled, scalar field. Applying the Brown-Ottewill-Page approximation [33] to adS space-time, the difference between the t.e.v. and the v.e.v. of the SET has the perfect fluid form with energy density E_β^{BOP}:

$$E_\beta^{BOP} = \frac{7\pi^2}{60\beta^4} \left(\cos\omega r\right)^4 \left[1 - \frac{5\omega^2\beta^2}{14\pi^2} - \frac{17\omega^4\beta^4}{112\pi^4}\right]. \tag{9.1}$$

While the Brown-Ottewill-Page approximation (9.1) does not exactly reproduce (6.26) for all values of the inverse temperature β, it does give the overall $\left(\cos\omega r\right)^4$ dependence

of (6.12, 6.26), as well as the perfect fluid form. Furthermore, it agrees with the high-temperature limit (8.17) of our exact QFT results up to $O([\omega\beta]^6)$.

For all values of the fermion mass, we find that the difference between the t.e.v.s and the v.e.v.s of all the quantities we have considered vanish on the space-time boundary, in both QFT and kinetic theory. Similar behaviour has been found for a massless, conformally coupled, scalar field in both pure adS [8] and for the renormalized vacuum polarization on a Schwarzschild-adS black hole background [34]. Furthermore, in the black hole case the value of the renormalized vacuum polarization on the space-time boundary matches that of the v.e.v. on pure adS space-time. We see that thermal radiation (whether produced by a black hole or in pure adS) tends to "clump" away from the boundary. This can be understood from the Tolman relation (7.4) for the local temperature, which vanishes as the boundary is approached.

While both the energy density E and pressure P vanish on the boundary, the equation of state $w = P/E$ can remain finite as the boundary is approached and has some interesting properties. In kinetic theory, w can take only two values on the boundary, either 1/3 for massless fermions or 0 for fermions of any nonzero mass. In QFT, w is again equal to 1/3 for massless fermions. For massive fermions, the QFT w on the boundary is independent of the inverse temperature β, and continuously decreases from 1/3 down to 0 as the fermion mass increases.

In this paper we have considered nonrotating thermal states on adS space-time. In the past few years, there has been renewed interest in the properties of rotating thermal fermion states, both within kinetic theory [18, 19] and in QFT on Minkowski space-time [35, 36, 37]. The properties of equilibrium states of gases undergoing rigid rotation in adS have been recently studied [18], focussing on the bulk viscosity. It would be interesting to extend our QFT analysis in this paper to rotating states for fermions on adS and compare with the kinetic theory results. On unbounded Minkowski space-time, it is known that rotating scalar and fermion fields have rather different properties [35]. In particular the only possible vacuum state for scalars is the nonrotating Minkowski vacuum, while for fermions a rotating vacuum can also be defined. This means that rotating thermal states for fermions can be defined, whereas for scalar fields rotating thermal states are ill-defined everywhere in the space-time. Rotating thermal states for fermions on unbounded Minkowski space-time are regular everywhere inside the speed-of-light (SOL) surface, where they diverge [35]. On adS, due to the time-like boundary, there may or may not be an SOL depending on the angular speed of rotation [18]. For a quantum scalar field, the only possible global vacuum state on adS is the nonrotating vacuum [38]. We conjecture that the situation for a quantum fermion field is likely to be different and expect to be able to define a rotating vacuum. If the angular speed is sufficiently small and there is no SOL, one might expect that rotating t.e.v.s for the fermion field would have some properties similar to those in bounded Minkowski space-time [36], while if there is an SOL, it seems likely that rotating t.e.v.s would diverge there, in analogy with the situation in unbounded Minkowksi space-time [35]. Testing these conjectures requires a full analysis of the QFT of rigidly-rotating fermions on adS,

to which we plan to return in a forthcoming publication.

Acknowledgments

Appendix A. Analytic expression for the bispinor of parallel transport

The bispinor of parallel transport $\Lambda(x, x')$ is the solution of (4.9) subject to the initial conditions (4.11). On adS space-time, $\Lambda(x, x')$ also satisfies (4.14). For later convenience, we introduce an auxiliary bispinor $\lambda(x, x')$ as follows:

$$\Lambda(x, x') = \frac{1}{\cos \frac{\omega s}{2} \sqrt{\cos \omega r \cos \omega r'}} \lambda(x, x'). \tag{A.1}$$

From (4.14) we deduce the following equations for $\lambda(x, x')$:

$$D_{\hat{\alpha}} \left[\frac{\lambda}{\sqrt{\cos \omega r \cos \omega r'}} \right] = \frac{\omega}{2} \tan \left(\frac{\omega s}{2} \right) \gamma_{\hat{\alpha}} \frac{\not{n}\lambda}{\sqrt{\cos \omega r \cos \omega r'}}, \tag{A.2}$$

$$D_{\hat{\alpha}'} \left[\frac{\lambda}{\sqrt{\cos \omega r \cos \omega r'}} \right] = \frac{\omega}{2} \tan \left(\frac{\omega s}{2} \right) \frac{\lambda}{\sqrt{\cos \omega r \cos \omega r'}} \not{n}'\gamma_{\hat{\alpha}'}, \tag{A.3}$$

and the initial conditions (4.11) become:

$$\lambda(x, x) = \cos \omega r, \qquad \overline{\lambda}(x, x') = \lambda(x', x),$$
$$\lambda(x, x')\lambda(x', x) = \cos^2 \frac{\omega s}{2} \cos \omega r \cos \omega r'. \tag{A.4}$$

The construction of the solution of (A.2, A.3) will be performed in four steps: (1) finding the time dependence of λ (Appendix A.1); (2) finding the radial dependence of λ (Appendix A.2); (3) simplifying the solution in terms of functions of the angular coordinates (Appendix A.3); and finally (4) determining the angular dependence of the remaining functions of the angular coordinates (Appendix A.4).

Appendix A.1. Time dependence

For the construction of $\lambda(x, x')$, both (A.2, A.3) need to be considered. For brevity, the details will be shown for (A.2) (which involves derivatives with respect to the unprimed indices). The analysis of (A.3) follows similarly.

The time dependence of λ can be determined by setting $\hat{\alpha} = \hat{0}$ in (A.2), yielding:

$$(\cos \omega \Delta t + C_\gamma) \partial_{\omega t/2} \lambda + \sin (\omega \Delta t) \lambda$$

$$= - \tan \left(\frac{\omega r}{2} \right) (\cos \omega r' + C_\gamma) \gamma^{\hat{0}} \frac{\boldsymbol{x} \cdot \boldsymbol{\gamma}}{r} \lambda - \sin (\omega r') \gamma^{\hat{0}} \frac{\boldsymbol{x'} \cdot \boldsymbol{\gamma}}{r'} \lambda, \tag{A.5}$$

where we have defined a quantity C_γ by

$$C_\gamma = \cos \omega r \cos \omega r' (1 - \cos \gamma \tan \omega r \tan \omega r'), \tag{A.6}$$

in terms of which the coefficient of $\partial_{\omega t/2}$ was obtained using the following relation:

$$\cos \omega r \cos \omega r' (1 + \cos \omega s) = \cos \omega \Delta t + C_\gamma. \tag{A.7}$$

To solve (A.5), it is convenient to cast it in the form:

$$\begin{pmatrix} A_t & B_t \\ B_t & A_t \end{pmatrix} \lambda(x, x') = 0, \tag{A.8}$$

where A_t and B_t are 2×2 matrices. Using the result

$$\begin{pmatrix} A & -B \\ -B & A \end{pmatrix} \begin{pmatrix} A & B \\ B & A \end{pmatrix} = \begin{pmatrix} A^2 - B^2 & [A, B] \\ [A, B] & A^2 - B^2, \end{pmatrix} \tag{A.9}$$

it can be seen that (A.8) can be diagonalised if A_t and B_t commute. The choice

$$A_t = (\cos \omega \Delta t + C_\gamma) \partial_{\omega t/2} + \sin \omega \Delta t,$$

$$B_t = \tan \left(\frac{\omega r}{2} \right) (\cos \omega r' + C_\gamma) \frac{\boldsymbol{x} \cdot \boldsymbol{\sigma}}{r} + \sin \omega r' \frac{\boldsymbol{x'} \cdot \boldsymbol{\sigma}}{r'}, \tag{A.10}$$

satisfies $[A_t, B_t] = 0$, since A_t is proportional to the 2×2 identity matrix and B_t has no time dependence. Squaring A_t and B_t from (A.10) gives:

$$A_t^2 = (\cos \omega \Delta t + C_\gamma)^2 \left[\frac{\partial^2}{\partial (\omega t/2)^2} + 1 \right] + 1 - C_\gamma^2,$$

$$B_t^2 = 1 - C_\gamma^2. \tag{A.11}$$

A similar analysis can be performed on (A.3). In this case a suitable choice of matrices $A_{t'}$ and $B_{t'}$ is

$$A_{t'} = \overleftarrow{\partial}_{\omega t'/2} (\cos \omega \Delta t + C_\gamma) - \sin \omega \Delta t,$$

$$B_{t'} = - \tan \left(\frac{\omega r'}{2} \right) (\cos \omega r + C_\gamma) \frac{\boldsymbol{x'} \cdot \boldsymbol{\sigma}}{r'} - \sin \omega r \frac{\boldsymbol{x} \cdot \boldsymbol{\sigma}}{r}, \tag{A.12}$$

so that:

$$\lambda(x, x') \begin{pmatrix} A_{t'} & B_{t'} \\ B_{t'} & A_{t'} \end{pmatrix} = 0. \tag{A.13}$$

The squares of $A_{t'}$ and $B_{t'}$ can be obtained from (A.11) by replacing $t \leftrightarrow t'$.

Therefore, $\lambda(x, x')$ obeys the following two differential equations:

$$\frac{\partial \lambda}{\partial (\omega t/2)^2} + \lambda = 0, \qquad \frac{\partial \lambda}{\partial (\omega t'/2)^2} + \lambda = 0, \tag{A.14}$$

so that $\lambda(x, x')$ is a harmonic function of $\omega t/2$ and $\omega t'/2$. Since in (A.1) the coordinates t and t' appear only through the combination $\Delta t = t - t'$, it can be assumed that λ depends on t and t' only through Δt.

For our later analysis, it is convenient to introduce the 2×2 constituents $\lambda_{ij} \equiv \lambda_{ij}(x, x')$ $(i, j = 1, 2)$ of λ by:

$$\lambda(x, x') = \begin{pmatrix} \lambda_{11}(x, x') & \lambda_{12}(x, x') \\ \lambda_{21}(x, x') & \lambda_{22}(x, x') \end{pmatrix}. \tag{A.15}$$

Since $\lambda(x, x')$ is a harmonic function of Δt, its constituents can be written as:

$$\lambda_{ij}(x, x') = \mathcal{C}_{ij} \cos \frac{\omega \Delta t}{2} + \mathcal{S}_{ij} \sin \frac{\omega \Delta t}{2}, \tag{A.16}$$

where the coefficients $\mathcal{C}_{ij}$ and $\mathcal{S}_{ij}$ are 2×2 matrices that depend only on $\boldsymbol{x}$ and $\boldsymbol{x}'$. In the coincidence limit, the second term above vanishes, while, from (A.4), $\mathcal{C}_{ij}$ should satisfy

$$\mathcal{C}_{ij}\rfloor_{\boldsymbol{x}'=\boldsymbol{x}} = \delta_{ij} \cos \omega r. \tag{A.17}$$

Appendix A.2. Radial dependence

The equation giving the dependence of λ on r can be obtained by multiplying (A.2) by $x^j \omega_j^{\hat{a}}/r$. After some rearrangement, we find the following relation:

$$\left[(\cos \omega \Delta t + C_\gamma) \partial_{\omega r/2} + \tan \frac{\omega r}{2} (\cos \omega r' + C_\gamma) \right.$$
$$\left. - \sin \omega r' \frac{\boldsymbol{x} \cdot \boldsymbol{\gamma}}{r} \frac{\boldsymbol{x}' \cdot \boldsymbol{\gamma}}{r'} - \sin \omega \Delta t \frac{\boldsymbol{x} \cdot \boldsymbol{\gamma}}{r} \gamma^{\hat{0}} \right] \lambda = 0. \tag{A.18}$$

The above equation can be brought into the form (A.8) by multiplying by

$$i\varepsilon_{ijk} x^i \gamma^{\hat{j}} \gamma^{\hat{k}}/2r = \begin{pmatrix} \boldsymbol{x} \cdot \boldsymbol{\sigma}/r & 0 \\ 0 & \boldsymbol{x} \cdot \boldsymbol{\sigma}/r \end{pmatrix}, \tag{A.19}$$

yielding:

$$A_r = \frac{\boldsymbol{x} \cdot \boldsymbol{\sigma}}{r} \left[(\cos \omega \Delta t + C_\gamma) \partial_{\omega r/2} + \tan \left(\frac{\omega r}{2} \right) (\cos \omega r' + C_\gamma) \right] + \frac{\boldsymbol{x}' \cdot \boldsymbol{\sigma}}{r'} \sin \omega r',$$
$$B_r = \sin \omega \Delta t. \tag{A.20}$$

After some algebra, it can be shown that:

$$A_r^2 = (\cos \omega \Delta t + C_\gamma)^2 \left[\frac{\partial^2}{\partial (\omega r/2)^2} + 1 \right] + \sin^2 \omega \Delta t, \tag{A.21}$$

while $B_r^2 = \sin^2 \omega \Delta t$. By applying the same methodology as in Appendix A.1, it can be shown that λ is a harmonic function of $\omega r/2$:

$$\frac{\partial^2 \lambda}{\partial (\omega r/2)^2} + \lambda = 0. \tag{A.22}$$

Employing the same method for the r' dependence, it can be shown that λ also satisfies:

$$\frac{\partial^2 \lambda}{\partial (\omega r'/2)^2} + \lambda = 0. \tag{A.23}$$

Equations (A.22–A.23) imply that λ is a harmonic function of both $\omega r/2$ and $\omega r'/2$. In particular, the 2×2 components λ_{ij}, as well as the matrices $\mathcal{C}_{ij}$ and $\mathcal{S}_{ij}$ (A.16) must also be harmonic functions of $\omega r/2$ and $\omega r'/2$. We therefore write $\mathcal{C}_{ij}$ and $\mathcal{S}_{ij}$ in the following form:

$$\mathcal{C}_{ij} = c_{ij}^{cc} \cos \frac{\omega r}{2} \cos \frac{\omega r'}{2} + c_{ij}^{cs} \cos \frac{\omega r}{2} \sin \frac{\omega r'}{2} + c_{ij}^{sc} \sin \frac{\omega r}{2} \cos \frac{\omega r'}{2} + c_{ij}^{ss} \sin \frac{\omega r}{2} \sin \frac{\omega r'}{2},$$

$$\mathcal{S}_{ij} = s_{ij}^{cc} \cos \frac{\omega r}{2} \cos \frac{\omega r'}{2} + s_{ij}^{cs} \cos \frac{\omega r}{2} \sin \frac{\omega r'}{2} + s_{ij}^{sc} \sin \frac{\omega r}{2} \cos \frac{\omega r'}{2} + s_{ij}^{ss} \sin \frac{\omega r}{2} \sin \frac{\omega r'}{2},$$

$$\text{(A.24)}$$

where the coefficients c_{ij}^{ab} and s_{ij}^{ab} depend only on the orientations $\boldsymbol{n} = \boldsymbol{x}/r$ and $\boldsymbol{n}' = \boldsymbol{x}'/r'$ of $\boldsymbol{x}$ and $\boldsymbol{x}'$. In other words, c_{ij}^{ab} and s_{ij}^{ab} depend only on the angular coordinates θ, θ', φ and φ'.

Appendix A.3. Simplifying the solution

We now simplify the expressions (A.15, A.16, A.24) for the auxiliary bispinor $\lambda(x, x')$ by finding relations between the coefficients c_{ij}^{ab} and s_{ij}^{ab} which will enable us to reduce the number of independent functions of the angular coordinates.

Some relations involving the terms in $\mathcal{C}_{11}$ and $\mathcal{S}_{11}$ can be obtained by considering the expression for the off-diagonal component λ_{21}, which can be obtained via (A.8):

$$\lambda_{21} = -B_t^{-1} A_t \lambda_{11}. \tag{A.25}$$

The operator A_t, defined in (A.10), has the following action on the harmonic functions of argument $\omega \Delta t/2$:

$$A_t \cos \frac{\omega \Delta t}{2} = \sin \left(\frac{\omega \Delta t}{2} \right) (1 - C_\gamma), \qquad A_t \sin \frac{\omega \Delta t}{2} = \cos \left(\frac{\omega \Delta t}{2} \right) (1 + C_\gamma), \tag{A.26}$$

where C_γ is defined in (A.6). Furthermore, the inverse of the matrix B_t (A.10) can be written as:

$$B_t^{-1} = \frac{1}{1 - C_\gamma^2} B_t. \tag{A.27}$$

Thus, λ_{21} takes the form:

$$\lambda_{21} = \mathcal{C}_{21} \cos \frac{\omega \Delta t}{2} + \mathcal{S}_{21} \sin \frac{\omega \Delta t}{2}$$

$$= -\left[\tan \left(\frac{\omega r}{2} \right) (\cos \omega r' + C_\gamma) \frac{\boldsymbol{x} \cdot \boldsymbol{\sigma}}{r} + \sin \omega r' \frac{\boldsymbol{x}' \cdot \boldsymbol{\sigma}}{r'} \right] \left(\frac{\mathcal{C}_{11} \sin \frac{\omega \Delta t}{2}}{1 + C_\gamma} + \frac{\mathcal{S}_{11} \cos \frac{\omega \Delta t}{2}}{1 - C_\gamma} \right).$$

$$\text{(A.28)}$$

When $r' = 0$, the expression (A.28) reduces to:

$$\lambda_{21}\rfloor_{r'=0} = -\frac{\boldsymbol{x} \cdot \boldsymbol{\sigma}}{r} \left[\sin \frac{\omega \Delta t}{2} \tan \frac{\omega r}{2} \left(c_{11}^{cc} \cos \frac{\omega r}{2} + c_{11}^{sc} \sin \frac{\omega r}{2} \right) \right.$$

$$\left. + \cos \frac{\omega \Delta t}{2} \cot \frac{\omega r}{2} \left(s_{11}^{cc} \cos \frac{\omega r}{2} + s_{11}^{sc} \sin \frac{\omega r}{2} \right) \right]. \tag{A.29}$$

Since $\lambda_{21}|_{r'=0}$ must be a harmonic function of $\omega r/2$, it follows that:

$$c_{11}^{sc} = s_{11}^{cc} = 0, \tag{A.30}$$

which holds for all $\boldsymbol{n}$ and $\boldsymbol{n}'$. In the case when $r = 0$, the expression (A.28) simplifies to:

$$\lambda_{21}|_{r=0} = -\frac{\boldsymbol{x}' \cdot \boldsymbol{\sigma}}{r'}\left[\sin\frac{\omega\Delta t}{2}\tan\frac{\omega r'}{2}\left(c_{11}^{cc}\cos\frac{\omega r'}{2} + c_{11}^{cs}\sin\frac{\omega r'}{2}\right)\right.$$
$$\left. + \cos\frac{\omega\Delta t}{2}\cot\frac{\omega r'}{2}s_{11}^{cs}\sin\frac{\omega r'}{2}\right], \tag{A.31}$$

implying that $c_{11}^{cs} = 0$.

We now consider the construction of λ_{21} using the radial matrices A_r and B_r:

$$\lambda_{21} = -B_r^{-1}A_r\lambda_{11}, \tag{A.32}$$

where $B_r^{-1} = 1/\sin\omega\Delta t$. The action of A_r (A.20) on harmonic functions of $\omega r/2$ is given by:

$$A_r\cos\frac{\omega r}{2} = \sin\left(\frac{\omega r}{2}\right)(-\cos\omega\Delta t + \cos\omega r')\frac{\boldsymbol{x}\cdot\boldsymbol{\sigma}}{r} + \cos\left(\frac{\omega r}{2}\right)\sin\omega r'\frac{\boldsymbol{x}'\cdot\boldsymbol{\sigma}}{r'},$$
$$A_r\sin\frac{\omega r}{2} = \cos\left(\frac{\omega r}{2}\right)(\cos\omega\Delta t + \cos\omega r')\frac{\boldsymbol{x}\cdot\boldsymbol{\sigma}}{r} - \sin\left(\frac{\omega r}{2}\right)\sin\omega r'\frac{\boldsymbol{x}\cdot\boldsymbol{\sigma}}{r}\frac{\boldsymbol{x}'\cdot\boldsymbol{\sigma}}{r'}\frac{\boldsymbol{x}\cdot\boldsymbol{\sigma}}{r}.$$
$$\tag{A.33}$$

To make use of the above properties, it is useful to write:

$$\lambda_{11} = C_{11}^r\cos\frac{\omega r}{2} + S_{11}^r\sin\frac{\omega r}{2}, \tag{A.34}$$

where

$$C_{11}^r = c_{11}^{cc}\cos\frac{\omega\Delta t}{2}\cos\frac{\omega r'}{2} + s_{11}^{cs}\sin\frac{\omega\Delta t}{2}\sin\frac{\omega r'}{2},$$
$$S_{11}^r = c_{11}^{ss}\cos\frac{\omega\Delta t}{2}\sin\frac{\omega r'}{2} + \sin\frac{\omega\Delta t}{2}\left(s_{11}^{sc}\cos\frac{\omega r'}{2} + s_{11}^{ss}\sin\frac{\omega r'}{2}\right). \tag{A.35}$$

Thus, λ_{21} can be written as:

$$\lambda_{21} = -\frac{1}{\sin\omega\Delta t}\left\{\left[\sin\left(\frac{\omega r}{2}\right)(-\cos\omega\Delta t + \cos\omega r')\frac{\boldsymbol{x}\cdot\boldsymbol{\sigma}}{r} + \cos\left(\frac{\omega r}{2}\right)\sin\omega r'\frac{\boldsymbol{x}'\cdot\boldsymbol{\sigma}}{r'}\right]C_{11}^r\right.$$
$$\left. + \left[\cos\left(\frac{\omega r}{2}\right)(\cos\omega\Delta t + \cos\omega r')\frac{\boldsymbol{x}\cdot\boldsymbol{\sigma}}{r} - \sin\left(\frac{\omega r}{2}\right)\sin\omega r'\frac{\boldsymbol{x}\cdot\boldsymbol{\sigma}}{r}\frac{\boldsymbol{x}'\cdot\boldsymbol{\sigma}}{r'}\frac{\boldsymbol{x}\cdot\boldsymbol{\sigma}}{r}\right]S_{11}^r\right\}. \tag{A.36}$$

In the limit $r = 0$, the above equation reduces to:

$$\lambda_{21}|_{r=0} = \sin\left(\frac{\omega\Delta t}{2}\right)\sin\left(\frac{\omega r'}{2}\right)\frac{\boldsymbol{x}\cdot\boldsymbol{\sigma}}{r}c_{11}^{ss}$$
$$- \cos\left(\frac{\omega\Delta t}{2}\right)\frac{\boldsymbol{x}\cdot\boldsymbol{\sigma}}{r}\left[\cos\left(\frac{\omega r'}{2}\right)s_{11}^{sc} + \sin\left(\frac{\omega r'}{2}\right)s_{11}^{ss}\right]$$
$$- \frac{1}{\sin\omega\Delta t}\left[\sin\omega r'\cos\left(\frac{\omega r'}{2}\right)\cos\left(\frac{\omega\Delta t}{2}\right)\left(\frac{\boldsymbol{x}'\cdot\boldsymbol{\sigma}}{r'}c_{11}^{cc} + \frac{\boldsymbol{x}\cdot\boldsymbol{\sigma}}{r}c_{11}^{ss}\right)\right.$$
$$\left. + \sin\frac{\omega\Delta t}{2}\sin\frac{\omega r'}{2}\sin\omega r'\left(\frac{\boldsymbol{x}'\cdot\boldsymbol{\sigma}}{r'}s_{11}^{cs} - \frac{\boldsymbol{x}\cdot\boldsymbol{\sigma}}{r}s_{11}^{sc} - \tan\left(\frac{\omega r'}{2}\right)\frac{\boldsymbol{x}\cdot\boldsymbol{\sigma}}{r}s_{11}^{ss}\right)\right]. \tag{A.37}$$

Since λ_{21} must be a harmonic function of $\omega \Delta t/2$, the coefficient of $1/\sin \omega \Delta t$ must vanish. Inside the square brackets, the coefficients of $\cos \frac{\omega \Delta t}{2}$ and $\sin \frac{\omega \Delta t}{2}$ must vanish individually, since they are linearly independent functions. Furthermore, $\sin \frac{\omega r'}{2} \sin \omega r' = (\cos \frac{\omega r'}{2} - \cos \frac{3\omega r'}{2})/2$ and $\sin \frac{\omega r'}{2} \sin \omega r' \tan \frac{\omega r'}{2} = (3 \sin \frac{\omega r'}{2} - \sin \frac{3\omega r'}{2})/2$ are also linearly independent, thus requiring that their coefficients vanish separately. Altogether, the following relations are obtained:

$$s_{11}^{ss} = 0, \qquad c_{11}^{ss} = -\frac{\boldsymbol{x} \cdot \boldsymbol{\sigma}}{r} \frac{\boldsymbol{x'} \cdot \boldsymbol{\sigma}}{r'} c_{11}^{cc}, \qquad s_{11}^{sc} = \frac{\boldsymbol{x} \cdot \boldsymbol{\sigma}}{r} \frac{\boldsymbol{x'} \cdot \boldsymbol{\sigma}}{r'} s_{11}^{cs}. \qquad (A.38)$$

Using the above information, (A.36) simplifies to:

$$\lambda_{21} = \cos\left(\frac{\omega \Delta t}{2}\right) \left[\sin\left(\frac{\omega r}{2}\right) \sin\left(\frac{\omega r'}{2}\right) \frac{\boldsymbol{x} \cdot \boldsymbol{\sigma}}{r} - \cos\left(\frac{\omega r}{2}\right) \cos\left(\frac{\omega r'}{2}\right) \frac{\boldsymbol{x'} \cdot \boldsymbol{\sigma}}{r'} \right] s_{11}^{cs}$$
$$- \sin\left(\frac{\omega \Delta t}{2}\right) \left[\sin\left(\frac{\omega r}{2}\right) \cos\left(\frac{\omega r'}{2}\right) \frac{\boldsymbol{x} \cdot \boldsymbol{\sigma}}{r} + \cos\left(\frac{\omega r}{2}\right) \sin\left(\frac{\omega r'}{2}\right) \frac{\boldsymbol{x'} \cdot \boldsymbol{\sigma}}{r'} \right] c_{11}^{cc}. \tag{A.39}$$

From the above analysis, we conclude that λ_{11} can be written using two unknown coefficients, namely c_{11}^{cc} and s_{11}^{cs}:

$$\lambda_{11} = \cos\left(\frac{\omega \Delta t}{2}\right) \left[\cos\left(\frac{\omega r}{2}\right) \cos\left(\frac{\omega r'}{2}\right) - \sin\left(\frac{\omega r}{2}\right) \sin\left(\frac{\omega r'}{2}\right) \frac{\boldsymbol{x} \cdot \boldsymbol{\sigma}}{r} \frac{\boldsymbol{x'} \cdot \boldsymbol{\sigma}}{r'} \right] c_{11}^{cc}$$
$$+ \sin\left(\frac{\omega \Delta t}{2}\right) \left[\cos\left(\frac{\omega r}{2}\right) \sin\left(\frac{\omega r'}{2}\right) + \sin\left(\frac{\omega r}{2}\right) \cos\left(\frac{\omega r'}{2}\right) \frac{\boldsymbol{x} \cdot \boldsymbol{\sigma}}{r} \frac{\boldsymbol{x'} \cdot \boldsymbol{\sigma}}{r'} \right] s_{11}^{cs}. \tag{A.40}$$

In (A.39, A.40) we have expressions for λ_{21} and λ_{11} in terms of two 2×2 matrices s_{11}^{cs} and c_{11}^{cc}, whose entries can only depend on $\boldsymbol{n}$ and $\boldsymbol{n'}$. In the following subsection, the angular dependence of these matrices will be determined by solving (A.2) directly.

Appendix A.4. Determining the functions of the angular coordinates

Having derived expressions for λ_{11} and λ_{21} in terms of s_{11}^{cs} and c_{11}^{cc}, we can now solve (A.2) for the left half of the matrix λ (A.15). However, before we can solve (A.2), we need to find $\not{n}\lambda$ and therefore we require the equivalent of (4.14) for $\not{n}\Lambda$. Using the following property:

$$D_{\hat{\alpha}} \not{n} = -A(n_{\hat{\alpha}} + \gamma_{\hat{\alpha}} \not{n}) \not{n}, \tag{A.41}$$

it can be shown that $\not{n}\Lambda$ satisfies the equation:

$$D_{\hat{\alpha}}(\not{n}\Lambda) = -\frac{A - C}{2}(n_{\hat{\alpha}} + \gamma_{\hat{\alpha}} \not{n})(\not{n}\Lambda). \tag{A.42}$$

Substituting (3.13) for A and C into (A.42) gives the equation

$$D_{\hat{\alpha}}(\not{n}\Lambda) = -\frac{\omega}{2} \cot\left(\frac{\omega s}{2}\right) (n_{\hat{\alpha}} + \gamma_{\hat{\alpha}} \not{n})(\not{n}\Lambda). \tag{A.43}$$

Using (A.1) to write (A.43) in terms of λ and taking advantage of the factor of $\cot \frac{\omega s}{2}$ on the right hand side, the following equation is obtained:

$$D_{\hat{\alpha}} \left[\cot\left(\frac{\omega s}{2}\right) \frac{\not{n}\lambda}{\sqrt{\cos \omega r \cos \omega r'}} \right] = -\frac{\omega}{2} \gamma_{\hat{\alpha}} \not{n} \left[\cot\left(\frac{\omega s}{2}\right) \frac{\not{n}\lambda}{\sqrt{\cos \omega r \cos \omega r'}} \right]. \tag{A.44}$$

The similarity between (A.2) and (A.44) enables the construction of $\not{n}\lambda$ directly. Indeed, using (3.9) for $n_{\hat{\alpha}}$ and (A.39, A.40) for λ_{21} and λ_{11}, a tedious but otherwise straightforward calculation allows $(\not{n}\lambda)_{11}$ to be written as:

$$
\frac{(\not{n}\lambda)_{11}}{\cot(\omega s/2)} = \sin\left(\frac{\omega\Delta t}{2}\right)\left[\cos\left(\frac{\omega r}{2}\right)\cos\left(\frac{\omega r'}{2}\right) + \sin\left(\frac{\omega r}{2}\right)\sin\left(\frac{\omega r'}{2}\right)\frac{\boldsymbol{x}\cdot\boldsymbol{\sigma}}{r}\frac{\boldsymbol{x}'\cdot\boldsymbol{\sigma}}{r'}\right]c_{11}^{cc}
$$
$$
- \cos\left(\frac{\omega\Delta t}{2}\right)\left[\cos\left(\frac{\omega r}{2}\right)\sin\left(\frac{\omega r'}{2}\right) - \sin\left(\frac{\omega r}{2}\right)\cos\left(\frac{\omega r'}{2}\right)\frac{\boldsymbol{x}\cdot\boldsymbol{\sigma}}{r}\frac{\boldsymbol{x}'\cdot\boldsymbol{\sigma}}{r'}\right]s_{11}^{cs},
$$
$$(\text{A.45})$$

while $(\not{n}\lambda)_{21}$ reduces to:

$$
\frac{(\not{n}\lambda)_{21}}{\cot(\omega s/2)} = \cos\left(\frac{\omega\Delta t}{2}\right)\left[\sin\left(\frac{\omega r}{2}\right)\cos\left(\frac{\omega r'}{2}\right)\frac{\boldsymbol{x}\cdot\boldsymbol{\sigma}}{r} - \cos\left(\frac{\omega r}{2}\right)\sin\left(\frac{\omega r'}{2}\right)\frac{\boldsymbol{x}'\cdot\boldsymbol{\sigma}}{r'}\right]c_{11}^{cc}
$$
$$
+ \sin\left(\frac{\omega\Delta t}{2}\right)\left[\sin\left(\frac{\omega r}{2}\right)\sin\left(\frac{\omega r'}{2}\right)\frac{\boldsymbol{x}\cdot\boldsymbol{\sigma}}{r} + \cos\left(\frac{\omega r}{2}\right)\cos\left(\frac{\omega r'}{2}\right)\frac{\boldsymbol{x}'\cdot\boldsymbol{\sigma}}{r'}\right]s_{11}^{cs}.
$$
$$(\text{A.46})$$

In order to solve (A.2), it is convenient to cast it in the following form:

$$
\frac{2}{\omega}\frac{\partial\lambda}{\partial x^i} + \frac{x^i}{r}\left\{\tan\left(\frac{\omega r}{2}\right)\lambda + \frac{1}{\cos\omega r}\left(1 - \frac{\sin\omega r}{\omega r}\right)\left[\tan\left(\frac{\omega r}{2}\right)\lambda - \frac{\boldsymbol{x}\cdot\boldsymbol{\gamma}}{r}\frac{\not{n}\lambda}{\cot(\omega s/2)}\right]\right\}
$$
$$
- \frac{\tan\omega r}{\omega r}\gamma^{\hat{i}}\frac{\boldsymbol{x}\cdot\boldsymbol{\gamma}}{r}\left[\tan\left(\frac{\omega r}{2}\right)\lambda - \frac{\boldsymbol{x}\cdot\boldsymbol{\gamma}}{r}\frac{\not{n}\lambda}{\cot(\omega s/2)}\right] = 0. \qquad (\text{A.47})
$$

It is sufficient to consider the (11) component of (A.47). Considering those terms proportional to $\cos\frac{\omega\Delta t}{2}$ and $\sin\frac{\omega\Delta t}{2}$ separately, we find:

$$
\partial_i c_{11}^{cc} = 0, \qquad \partial_i s_{11}^{cs} = 0, \qquad (\text{A.48})
$$

thus showing that c_{11}^{cc} and s_{11}^{cs} are constants. In the coincidence limit, λ_{11} and λ_{21} reduce to:

$$
\lambda_{11}\big|_{x=x'} = (\cos\omega r)c_{11}^{cc}, \qquad \lambda_{21}\big|_{x=x'} = -(\cos\omega r)\left(\frac{\boldsymbol{x}\cdot\boldsymbol{\sigma}}{r}\right)s_{11}^{cs}. \qquad (\text{A.49})
$$

According to (A.4), in the coincidence limit $\lim_{x'\to x}\lambda(x,x') = \cos\omega r$, from which we determine the constants c_{11}^{cc} and s_{11}^{cs} to be:

$$
c_{11}^{cc} = 1, \qquad s_{11}^{cs} = 0. \qquad (\text{A.50})
$$

This result allows us to write (A.39, A.40) as:

$$
\lambda_{11} = \cos\left(\frac{\omega\Delta t}{2}\right)\left[\cos\left(\frac{\omega r}{2}\right)\cos\left(\frac{\omega r'}{2}\right) - \sin\left(\frac{\omega r}{2}\right)\sin\left(\frac{\omega r'}{2}\right)\frac{\boldsymbol{x}\cdot\boldsymbol{\sigma}}{r}\frac{\boldsymbol{x}'\cdot\boldsymbol{\sigma}}{r'}\right], \qquad (\text{A.51})
$$

$$
\lambda_{21} = -\sin\left(\frac{\omega\Delta t}{2}\right)\left[\sin\left(\frac{\omega r}{2}\right)\cos\left(\frac{\omega r'}{2}\right)\frac{\boldsymbol{x}\cdot\boldsymbol{\sigma}}{r} + \cos\left(\frac{\omega r}{2}\right)\sin\left(\frac{\omega r'}{2}\right)\frac{\boldsymbol{x}'\cdot\boldsymbol{\sigma}}{r'}\right]. \qquad (\text{A.52})
$$

The 2×2 component λ_{12} can be found by using the second property (A.4):

$$
\lambda_{12}(x,x') = -\lambda_{21}^{\dagger}(x',x) = \lambda_{21}(x,x'). \qquad (\text{A.53})
$$

Finally, λ_{22} can be found from λ_{12} via (A.8):

$$
\lambda_{22}(x,x') = -B_t^{-1}A_t\lambda_{12}, \qquad (\text{A.54})
$$

and hence we have

$$\lambda_{22}(x, x') = \lambda_{11}(x, x'). \tag{A.55}$$

It can be checked that introducing (A.51–A.55) into (A.15) and using (A.1) to find $\Lambda(x, x')$ recovers (4.15).

Finally, the (12) and (22) components of $\slashed{n}\lambda$ can be found starting from (A.53, A.55):

$$(\slashed{n}\lambda)_{12} = -(\slashed{n}\lambda)_{21}, \qquad (\slashed{n}\lambda)_{22} = -(\slashed{n}\lambda)_{11}, \tag{A.56}$$

thus establishing (4.16).

References

[1] Gubser S S, Klebanov I R and Polyakov A M 1998 *Phys. Lett.* B **428** 105–14
   Maldacena J M 1999 *Int. J. Theor. Phys.* **38** 1113–33
   Witten E 1998 *Adv. Theor. Math. Phys.* **2** 253–91
[2] Aharony O, Gubser S S, Maldacena J M, Ooguri H and Oz Y 2000 *Phys. Rept.* **323** 183–386
[3] Avis S J, Isham C J and Storey D 1978 *Phys. Rev.* D **18** 3565–76
[4] Burgess C P and Lütken C A 1985 *Phys. Lett.* B **153** 137–41
   Cotăescu I I 1999 *Phys. Rev.* D **60** 107504
[5] Kent C and Winstanley E 2015 *Phys. Rev.* D **91** 044044
[6] Camporesi R and Higuchi A 1992 *Phys. Rev.* D **45** 3591–603
[7] Caldarelli M M 1999 *Nucl. Phys.* B **549** 499–515
[8] Allen B, Folacci A and Gibbons G W 1987 *Phys. Lett.* B **189** 304–10
[9] Allen B and Jacobson T 1986 *Commun. Math. Phys.* **103** 669–92
[10] Belokogne A, Folacci A and Queva J 2016 *Phys. Rev.* D **94** 105028
[11] Allen B and Lütken C A 1986 *Commun. Math. Phys.* **106** 201–10
[12] Mück W 2000 *J. Phys. A: Math. Gen.* **33** 3021–6
[13] Cotăescu I I 2007 *Rom. J. Phys.* **52** 895–940
[14] Ambruş V E and Winstanley E 2015 *Phys. Lett.* B **749** 597–602
[15] Buhl-Mortensen I, de Leeuw M, Ipsen A C, Kristjansen C and Wilhelm M 2017 *J. High Energy Phys.* **1701** 098
[16] Tolman R C 1930 *Phys. Rev.* **35** 904–24
   Tolman R C and Ehrenfest P 1930 *Phys. Rev.* **36** 1791–8
[17] Décanini Y and Folacci A 2008 *Phys. Rev.* D **78** 044025
[18] Ambruş V E and Cotăescu I I 2016 *Phys. Rev.* D **94** 085022
[19] Ambruş V E and Blaga R 2015 *Annals of West University of Timişoara - Physics* **58** 89–108
[20] Florkowski W and Maksymiuk E 2015 *J. Phys. G: Nucl. Part. Phys.* **42** 045106
[21] Brill D R and Wheeler J A 1957 *Rev. Mod. Phys.* **29** 465–79
   Weldon H A 2001 *Phys. Rev.* D **63** 104010
   Gies H and Lippoldt S 2014 *Phys. Rev.* D **89** 064040
[22] Christensen S M 1976 *Phys. Rev.* D **14** 2490–501
[23] Poisson E 2004 *Class. Quantum Grav.* **21** R153–232
[24] Christensen S M 1978 *Phys. Rev.* D **17** 946–963
[25] Groves P B, Anderson P R and Carlson E D 2002 *Phys. Rev.* D **66** 124017
[26] Birrell N D and Davies P C W 1982 *Quantum fields in curved space* (Cambridge: Cambridge University Press).
[27] Rezzolla L and Zanotti O 2013 *Relativistic hydrodynamics* (Oxford: Oxford University Press)
[28] Cardall C Y, Endeve E and Mezzacappa A 2013 *Phys. Rev.* D **88** 023011

[29] Cercignani C and Kremer G M 2002 *The relativistic Boltzmann equation: theory and applications* (Basel: Birkhäuser)

[30] Ambruș V E 2014 *Dirac fermions on rotating space-times* (PhD thesis, University of Sheffield) [http://etheses.whiterose.ac.uk/id/eprint/7527]

[31] Olver F W J, Lozier D W, Boisvert R F and Clark C W 2010 *NIST Handbook of Mathematical Functions* (New York: Cambridge University Press)

[32] Gibbons G W and Hawking S W 1977 *Phys. Rev.* D **15** 2738–51

[33] Brown M R, Ottewill A C and Page D N 1986 *Phys. Rev.* D **33** 2840–50

[34] Flachi A and Tanaka T 2008 *Phys. Rev.* D **78** 064011

[35] Ambruș V E and Winstanley E 2014 *Phys. Lett.* B **734** 296–301

[36] Ambruș V E and Winstanley E 2016 *Phys. Rev.* D **93** 104014

[37] Manning A 2015 Fermions in rotating reference frames `arXiv:1512.00579 [hep-th]`
     Ebihara S, Fukushima K and Mameda K 2017 *Phys. Lett.* B **764** 94–9
     Chernodub M N and Gongyo S 2017 *J. High Energy Phys.* **1701** 136
     Chernodub M N and Gongyo S 2017 *Phys. Rev.* D **95** 096006

[38] Kent C and Winstanley E 2015 *Phys. Lett.* B **740** 188–91